

Comparison of H–H versus Si–H σ -Bond Coordination and Activation on 16e Metal Fragments. Organosilane, N₂, and Ethylene Addition to the Agostic Complex W(CO)₃(PR₃)₂ and Dynamic NMR Behavior of the Latter

Matthew D. Butts, Jeffrey C. Bryan, Xiao-Liang Luo, and Gregory J. Kubas*

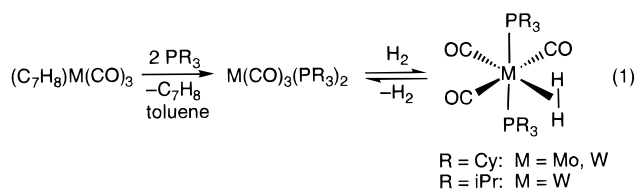
Chemical Science and Technology Division, MS J514, Los Alamos National Laboratory, Los Alamos, New Mexico 87545

Received July 23, 1996[⊗]

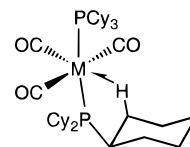
Variable-temperature ³¹P{¹H} NMR spectroscopy of the agostic complexes M(CO)₃(PCy₃)₂ (M = Mo, W) indicates dynamic behavior as evidenced by collapse below –20 °C of a singlet to an AB signal plus a shifted singlet. The inequivalency of the phosphines is possibly due to the presence of conformational isomers resulting from hindered rotation of the M–P bond or, less likely, a geometric isomer with pseudo-*cis* PCy₃ ligands. Further studies on the coordination chemistry of W(CO)₃(PR₃)₂ (R = iPr, Cy) were performed. The bridging dinitrogen complex [W(CO)₃(PiPr₃)₂]₂(μ -N₂) (**1**) was cleanly formed in the reaction of W(CO)₃(PiPr₃)₂ with N₂. Complex **1** was structurally characterized and compared with other bridging dinitrogen compounds of tungsten. The ethylene complex W(CO)₃(PCy₃)₂(η^2 -C₂H₄) (**2**) was synthesized and characterized by X-ray crystallography in order to compare the binding mode of ethylene with that of H₂. Phenylsilane reacted with W(CO)₃(PR₃)₂ (R = iPr, Cy) to form the thermally unstable oxidative addition (OA) products WH(SiH₂Ph)(CO)₃(PR₃)₂ (**3**, R = Cy; **4**, R = iPr). Diphenylsilane reacted with W(CO)₃(PiPr₃)₂ at 60 °C to form the bridging silyl species [W(CO)₃(PiPr₃)]₂(μ -SiHPh₂)₂ (**5**), which was confirmed by spectroscopic techniques and X-ray crystallography to have two 3-center 2-electron W···H···Si interactions. Detailed comparisons of the binding and activation of silanes versus H₂ on various 16e metal centers suggest a high degree of similarity, but relative ease of OA depends on the electrophilicity of the metal–ligand fragment and other factors such as bond energetics. Increasing the electrophilicity of the metal center (e.g., adding positive charge) may aid in stabilizing alkane coordination.

Introduction

The role of metal to ligand back-bonding in the coordination chemistry of strong π -acceptor ligands such as CO, ethylene, and dinitrogen has long been established but is only now being defined in the activation of σ -bonded ligands such as H₂ and silanes. A massive amount of experimental and theoretical data for the binding and oxidative addition of these and related ligands on a wide array of transition metal fragments has been accumulated within the past 10 years. Key to the development of this field has been the creation of new unsaturated 5-coordinate precursors (including Cp and Tp systems) which often can be isolated and bind sixth ligands reversibly. In early studies of group 6 complexes, we found that the addition of trialkylphosphines, PR₃, with large cone angles (R = iPr, Cy) to (C₇H₈)M(CO)₃ (M = Mo, W; C₇H₈ = cycloheptatriene) under an atmosphere of H₂ resulted in the formation of M(CO)₃(PR₃)₂(H₂), the first characterized examples of η^2 -H₂ coordination to a metal center (eq 1).¹ These reactions were found to proceed



through the intermediate M(CO)₃(PR₃)₂ complexes.^{1a,2,3} X-ray crystallographic studies performed on the Cr² and W³ complexes M(CO)₃(PR₃)₂ (M = Cr, R = Cy; M = W, R = iPr, Cy) indicated that these species were in essence 6-coordinate complexes with one metal site occupied by an agostic^{1g,4} C–H bond of a phosphine ligand.



The same is believed to be true in the molybdenum analogues, which like W(CO)₃(PR₃)₂ displayed reduced ν (CH) due to the agostic C–H in the range 2540–2710 cm⁻¹.³

These species can be likened to low-temperature-stable alkane adducts of often studied photochemically-generated M(CO)₅ fragments,⁵ but they are stabilized entropically because the agostic interaction is intramolecular and also presumably electronically by the electron-donating phosphines. In the latter regard, σ -bond interactions with metals are anchored by three-center bonding but are greatly reinforced by metal d π to X–H σ^* back-bonding. Back-bonding is favored by increasing the electron richness of the metal center by electron-donating ligands. Most

- (1) (a) Kubas, G. J. *J. Chem. Soc., Chem. Commun.* **1980**, 61. (b) Kubas, G. J.; Ryan, R. R.; Swanson, B. I.; Vergamini, P. J.; Wasserman, H. *J. Am. Chem. Soc.* **1984**, *106*, 451. (c) Kubas, G. J.; Unkefer, C. J.; Swanson, B. I.; Fukushima, E. *J. Am. Chem. Soc.* **1986**, *108*, 7000. (d) Kubas, G. J. *Acc. Chem. Res.* **1988**, *21*, 120. Recent reviews: (e) Jessup, P. G.; Morris, R. H. *Coord. Chem. Rev.* **1992**, *121*, 155. (f) Heinekey, D. M.; Oldham, W. J., Jr. *Chem. Rev.* **1993**, *93*, 913. (g) Crabtree, R. H. *Angew. Chem., Int. Ed. Engl.* **1993**, *32*, 789. (h) Morris, R. H. *Can. J. Chem.* **1996**, *74*, 1907.
- (2) Zhang, K.; Gonzalez, A. A.; Mukerjee, S. L.; Chou, S.-J.; Hoff, C. D.; Kubat-Martin, K. A.; Barnhart, D.; Kubas, G. J. *J. Am. Chem. Soc.* **1991**, *113*, 9170. The Cr complex was prepared from Cr(CO)₃(naphthalene); Gonzalez, A. A.; Mukerjee, S. L.; Chou, S.-L.; Zhang, K.; Hoff, C. D. *J. Am. Chem. Soc.* **1988**, *110*, 4419.
- (3) Wasserman, H. J.; Kubas, G. J.; Ryan, R. R. *J. Am. Chem. Soc.* **1986**, *108*, 2294. For improved syntheses of M(CO)₃(PCy₃)₂ and precursors, see: Kubas, G. J. *Organomet. Synth.* **1986**, *3*, 254; *Inorg. Synth.* **1990**, *27*, 1.
- (4) Brookhart, M.; Green, M. L. H.; Wong, L.-L. *Prog. Inorg. Chem.* **1988**, *36*, 1.

[⊗] Abstract published in *Advance ACS Abstracts*, June 15, 1997.

Table 1. Types of Coordination and Reactivity with $W(CO)_3(PR_3)_2^a$

	reactn with	no reactn with
irreversible binding	SO ₂ , CO	CO ₂ , Xe
	NH ₃ , RNH ₂ , py	R ₃ N, R ₂ NH
	CH ₃ CN, DMF	alkanes, arenes
	PR ₃ , P(OR) ₃	large PR ₃
reversible binding	H ₂ , N ₂ , C ₂ H ₄	propylene, C ₂ F ₄
	H ₂ O, ^b ROH, R ₂ C=O	
	tetrahydrofuran	furan
	R ₂ S, thiophene	R ₂ O
oxidative addition	H ₂ (equil), SiH ₃ Ph	
	HX (X = Cl, BF ₄) ^c	
free radical formation	RSH, ^d H ₂ S ^d	
	I ₂ , ^d RSSR ^d	

^a This work and refs 2a and 3 unless noted. ^b Reference 18a. ^c Reference 31. ^d Reference 55.

importantly, increased back-bonding weakens and eventually cleaves the σ -bond, so there is a crucial but enigmatic fine balance of σ donation and π back-donation that needs to be defined in order to fully understand σ -bond activation. An effective course to follow is to characterize a large series of complexes, varying the electronic properties of both the metal–ligand set and the substrate (sixth ligand). This approach will elucidate the electronic structure requirements for the optimal design of metal fragments for σ -bond activation, possibly even leading to the elusive stabilization of metal–alkane complexes.

The agostic C–H···M interactions in $M(CO)_3(PR_3)_2$ ($M = Cr, Mo, W$; $R = Cy, iPr$) have been shown to be easily displaced by a large variety of small molecules.^{1a,2,3,6} Four different types of binding and/or reactivity have now been observed as summarized in Table 1, including oxidative addition and in some cases unanticipated formation of stable 17e free radicals, $W(CO)_3(PR_3)_2(L)$ ($L = I, SR$). In certain instances, the large phosphines sterically inhibit ligand binding to a fine degree (e.g., NH₂Me binds but NHMe₂ does not), but for the most part electronics determine type of reactivity. This paper reports further investigation of the coordination chemistry of the tungsten complexes with strong π -acceptor ligands such as ethylene, dinitrogen, and silanes where back-bonding is a key component of the interaction as for η^2 -H₂. In contrast to H₂, organosilanes have been found to undergo complete oxidative addition to $W(CO)_3(PR_3)_2$. Comparison of the binding and ease of oxidative addition of silanes versus H₂ can now be made for a large series of d⁶ group 6–8 metal complexes and is reported here also.

As an additional feature for study, the agostic complexes $M(CO)_3(PR_3)_2$ were early found to be highly fluxional in

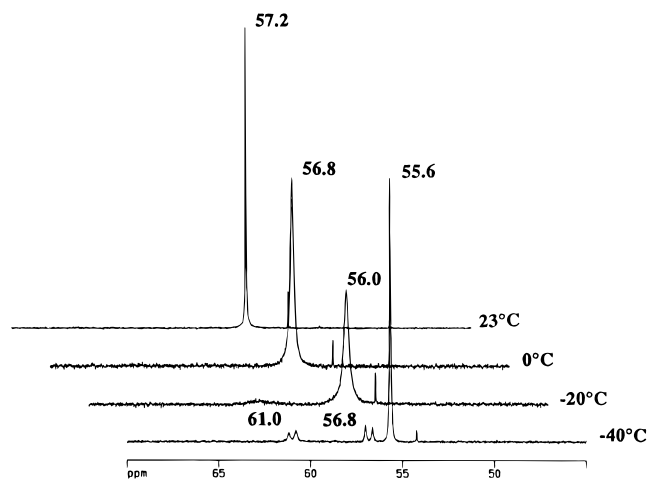


Figure 1. Variable-temperature $^{31}P\{^1H\}$ NMR spectra (202.46 MHz) of $Mo(CO)_3(PCy_3)_2$ in toluene- d_8 under helium. The weak singlet near 54 ppm was unidentified.

solution whereby only a single resonance was observed in the respective $^{31}P\{^1H\}$ NMR spectra, and the agostic hydrogens could not be resolved by 1H NMR spectroscopy at any accessible temperature.³ We have now further investigated the solution behavior of the W and Mo complexes $M(CO)_3(PCy_3)_2$ by low-temperature $^{31}P\{^1H\}$ and 1H NMR spectroscopy with the goal of better understanding the nature of the C–H···M interaction.

Results and Discussion

Temperature-Dependent Behavior of the Agostic Complexes $M(CO)_3(PR_3)_2$. Because the energy of the agostic interaction in $M(CO)_3(PR_3)_2$ is a crucial parameter in determination of binding energies of H₂ and other ligands (eq 1),⁶ attempts have been made to obtain this value using NMR methods. However, the interaction is so dynamic that a static agostic structure could not be frozen out by NMR, although unusual temperature-dependent behavior was nonetheless observed. The low-temperature ($-40^\circ C$) $^{31}P\{^1H\}$ NMR spectrum of $Mo(CO)_3(PCy_3)_2$ in toluene- d_8 contained two doublets of equal intensity (AB pattern) at 61.0 and 56.8 ppm ($J_{PP} = 77$ Hz) and a singlet at 55.6 ppm (Figure 1). On gradual warming, these resonances coalesced (reversibly) to a single broad peak which sharpened on further warming to room temperature (57.2 ppm). The 1H NMR spectrum at low temperature contained only broad resonances between 1 and 2 ppm attributed to the cyclohexyl groups. Similar behavior was observed for $W(CO)_3(PCy_3)_2$ except that at low temperature ($-60^\circ C$) only one doublet of the AB pattern was observed (59.9 ppm, $J = 81$ Hz) together with a broad singlet at 53.0 ppm (Figure 2). It is likely that the other doublet is buried under the broad singlet. Once again, the 1H NMR spectrum at $-60^\circ C$ contained only resonances for the cyclohexyl groups. The spectra of both $M(CO)_3(PCy_3)_2$ compounds as a function of temperature were indistinguishable from those of $M(CO)_3[P(Cy-d_{11})_3]_2$ ($M = Mo, W$) in toluene- d_8 .

Because of the similarities in the variable-temperature NMR spectroscopic characteristics, it seems likely that the phenomenon that gives rise to the new ^{31}P signals is common to both the Mo and W complexes, $M(CO)_3(PCy_3)_2$ and also to $[Re(CO)_3(PCy_3)_2]BAR_4$, reported by Heinekey and co-workers to undergo analogous behavior.⁷ Proving the origin of the AB

- (5) (a) Graham, M. A.; Perutz, R. N.; Poliakov, M.; Turner, J. J. *J. Organomet. Chem.* **1972**, *34*, C34. (b) Perutz, R. N.; Turner, J. J. *J. Am. Chem. Soc.* **1975**, *97*, 4791. (c) Brown, C. E.; Ishikawa, Y.; Hackett, P. A.; Rayner, D. M. *J. Am. Chem. Soc.* **1990**, *112*, 2530 and references therein. (d) Andrea, R. R.; Vuurman, M. A.; Stufkens, D. J.; Oskam, A. *Recl. Trav. Chim. Pays-Bas* **1986**, *105*, 372. (e) Church, S. P.; Grevels, F.-W.; Hermann, H.; Shaffner, K. *J. Chem. Soc., Chem. Commun.* **1985**, 30. (f) Upmacis, R. K.; Gadd, G. E.; Poliakov, M.; Simpson, M. B.; Turner, J. J.; Whyman, R.; Simpson, A. F. *J. Chem. Soc., Chem. Commun.* **1985**, 27. (g) Sweany, R. L. *J. Am. Chem. Soc.* **1985**, *107*, 2374. (h) Upmacis, R. K.; Poliakov, M.; Turner, J. J. *J. Am. Chem. Soc.* **1986**, *108*, 3645. (i) Hall, C.; Perutz, R. N. *Chem. Rev.* **1996**, *96*, 3125. (j) Walsh, E. F.; Popov, V. K.; George, M. W.; Poliakov, M. *J. Phys. Chem.* **1995**, *99*, 12016. (k) Ishikawa, Y.; Hackett, P. A.; Rayner, D. M. *J. Phys. Chem.* **1989**, *93*, 652.
- (6) (a) Zhang, K.; Gonzalez, A. A.; Hoff, C. D. *J. Am. Chem. Soc.* **1989**, *111*, 3627. (b) Gonzalez, A. A.; Zhang, K.; Nolan, S. P.; de la Vega, R. L.; Mukerjee, S. L.; Hoff, C. D.; Kubas, G. J. *Organometallics* **1988**, *7*, 2429. (c) Gonzalez, A. A.; Zhang, K.; Mukerjee, S. L.; Hoff, C. D.; Khalsa, G. R. K.; Kubas, G. J. *ACS Symp. Ser.* **1990**, *428*, 133. (d) Kubas, G. J.; Nelson, J. E.; Bryan, J. C.; Eckert, J.; Wisniewski, L.; Zilm, K. *Inorg. Chem.* **1994**, *33*, 2954.

- (7) (a) Heinekey, D. M.; Schomber, B. M.; Radzewich, C. E. *J. Am. Chem. Soc.* **1994**, *116*, 4515. (b) Heinekey, D. M.; Radzewich, C. E.; Voges, M. H.; Schomber, B. M. *J. Am. Chem. Soc.* **1997**, *119*, 4172.

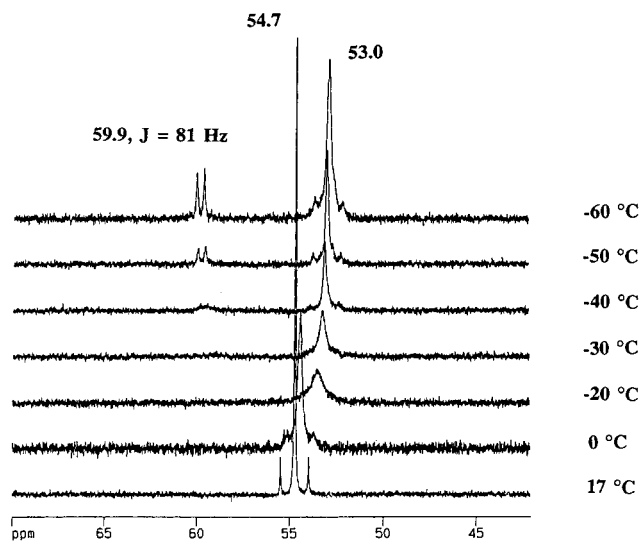
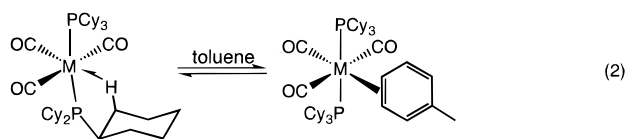


Figure 2. Variable-temperature $^{31}\text{P}\{^1\text{H}\}$ NMR spectra (202.46 MHz) of $\text{W}(\text{CO})_3(\text{PCy}_3)_2$ in toluene- d_8 under helium.

spectrum is difficult, but several possibilities can be eliminated, including that it represents the static agostic complex, which does contain inequivalent phosphines. This assignment is very unlikely because the agostic C–H was not observed in the ^1H NMR spectrum for any of the complexes at any temperature. Agostic hydrogens are typically shifted significantly upfield (relative to the geminal nonagostic hydrogens) in cases where static agostic complexes have been characterized by low-temperature NMR.⁸ Most importantly, the coalescence temperature, which is near -10°C for both the W and Mo complexes, is far too high for freezing out such a highly dynamic weak interaction (binding enthalpy is estimated^{6b,c} to be ca 10–15 kcal/mol). Typically temperatures below -80°C are required to observe static agostic structures,⁴ and decoalescence occurs at -90°C for the aryl C–H \cdots Mo interaction in $\text{Mo}(\text{CO})(\text{Bz}_2\text{PC}_2\text{H}_4\text{PBz}_2)_2$.^{8j} The lack of resonances in the hydride region of the ^1H NMR also argues against the presence of phosphine cyclometalation structures, i.e. scission of the C–H bond to form M–C and M–H bonds.

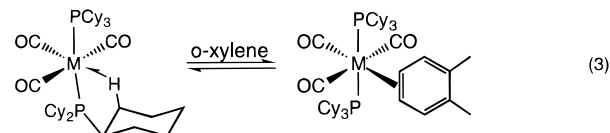
A third explanation for the AB pattern could be an equilibrium solvent-bound species (eq 2). The toluene- d_8 solvent would



have to be bound asymmetrically with respect to the phosphines, e.g. η^2 along the P–M–P axis (η^6 - or η^4 -arene binding is prohibited due to steric crowding). In the unlikely event that

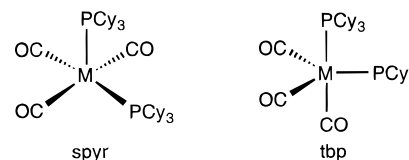
(8) (a) Carr, N.; Mole, L.; Orpen, A. G.; Spencer, J. L. *J. Chem. Soc., Dalton Trans.* **1992**, 2653. (b) Conroy-Lewis, F. M.; Mole, L.; Redhouse, A. D.; Litster, S. A.; Spencer, J. L. *J. Chem. Soc., Chem. Commun.* **1991**, 1601. (c) Brookhart, M.; Lincoln, D. M.; Bennett, M. A.; Pelling, S. *J. Am. Chem. Soc.* **1990**, *112*, 2691. (d) Ozawa, F.; Park, J. W.; Mackenzie, P. B.; Schaefer, W. P.; Henling, L. M.; Grubbs, R. H. *J. Am. Chem. Soc.* **1989**, *111*, 1319. (e) Park, J. W.; Mackenzie, P. B.; Schaefer, W. P.; Grubbs, R. H. *J. Am. Chem. Soc.* **1986**, *108*, 6402. (f) Benn, R.; Holle, S.; Jolly, P. W.; Mynott, R.; Romao, C. C. *Angew. Chem., Int. Ed. Engl.* **1986**, *25*, 555. (g) Cracknell, R. B.; Orpen, A. G.; Spencer, J. L. *J. Chem. Soc., Chem. Commun.* **1986**, 1005. (h) Cracknell, R. B.; Orpen, A. G.; Spencer, J. L. *J. Chem. Soc., Chem. Commun.* **1984**, 326. (i) Brookhart, M.; Green, M. L. H.; Pardy, R. B. A. *J. Chem. Soc., Chem. Commun.* **1983**, 691. (j) Luo, X.-L.; Kubas, G. J.; Burns, C. J.; Eckert, J. *Inorg. Chem.* **1994**, *33*, 5219.

this is sterically allowed, one would then expect *o*-xylene to form a similar complex, but with equivalent phosphine environments (eq 3). However, the same spectrum was observed for



$\text{Mo}(\text{CO})_3(\text{PCy}_3)_2$ in an *o*-xylene solvent mixture (hexane and Et_2O added to prevent freezing). Solvent binding (CH_2Cl_2) was not seen for $[\text{Re}(\text{CO})_3(\text{PCy}_3)_2]^+$ either.⁷ Importantly, none of the three scenarios considered thus far explain the observation of the singlet resonance found in the low-temperature ^{31}P NMR spectra of each complex (Mo = 55.6 ppm, s, Figure 1; W = 53.0 ppm, br s, Figure 2; $\text{Re}^+ = 24.0$ ppm⁷, br).

A fourth possibility is that an equilibrium exists between the agostic complex, in which the C–H \cdots M interaction is too dynamic to be observed in the slow exchange regime (producing the singlet peak), and an isomer which has inequivalent phosphines coupled to each other (giving the AB pattern). Square pyramidal (spyr) or trigonal bipyramidal (tbp) species with *cis*-phosphines and no agostic interaction are candidates:



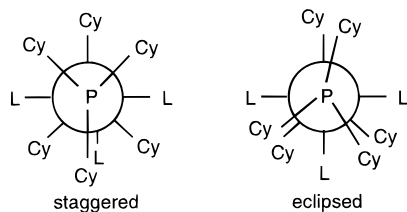
Closely-related $\text{Re}(\text{CO})_3(\text{PCy}_3)_2$ was in fact found by crystallography to have a distorted spyr structure with no agostic interaction,⁹ although this is a 17e radical with chemically equivalent *trans* phosphines. The 16e species $\text{TcCl}(\text{dpe})_2$ and $[\text{MCl}(\text{R}_2\text{PCH}_2\text{PR}_2)_2]^+$ (M = Ru, Os) have distorted tbp structures,¹⁰ although here the coordinative unsaturation is stabilized by π -donation from chloride¹¹ and chelating phosphines and no carbonyls are present. Low-spin d^6 metal systems normally display the most pronounced preference for the spyr structure, with preference for π -accepting ligands in the basal position.¹² Despite the large bulk of the PCy_3 ligand and common belief, *cis*-(PCy_3) $_2\text{ML}_n$ compounds have been characterized,¹³ including *cis*- $\text{Mo}(\text{CO})_4(\text{PCy}_3)_2$.^{13c} Thus *cis* structures for $\text{M}(\text{CO})_3(\text{PCy}_3)_2$ are possible, and the spyr geometry should be electronically and sterically favored over the tbp form.

However, the above rationale is problematic also. The coupling constants, $J_{\text{pp}} = 77$ and 81 Hz, were more consistent with *trans*- than with *cis*- PR_3 , near those measured for

(9) Crocker, L. S.; Heinekey, D. M.; Schultz, G. K. *J. Am. Chem. Soc.* **1989**, *111*, 405.
 (10) (a) Burrell, A. K.; Bryan, J. C.; Kubas, G. J. *J. Am. Chem. Soc.* **1994**, *116*, 1575. (b) Mezzetti, A.; Del Zotto, A.; Rigo, P.; Pahor, N. B. *J. Chem. Soc. Dalton Trans.* **1989**, 1045. (c) Chin, B.; Lough, A. J.; Morris, R. H.; Schweitzer, C.; D'Agostino, C. *Inorg. Chem.* **1994**, *33*, 6278. (d) Lough, A. J.; Morris, R. H.; Schlaf, M. *Acta Crystallogr., Sect. C* **1996**, *C52*, 2193.
 (11) Caulton, K. G. *New J. Chem.* **1994**, *18*, 25 and references therein.
 (12) (a) Pearson, R. G. *J. Am. Chem. Soc.* **1969**, *91*, 4947. (b) Rossi, A. R.; Hoffmann, R. *Inorg. Chem.* **1975**, *14*, 365. (c) Hoffman, P. R.; Caulton, K. G. *J. Am. Chem. Soc.* **1975**, *97*, 4221. (d) Albright, T. A.; Burdett, J. K.; Whangbo, M. H. *Orbital Interactions in Chemistry*; John Wiley & Sons: New York, 1985; pp 313–326.
 (13) (a) Grumbine, S. D.; Tilley, T. D.; Arnold, F. P.; Rheingold, A. L. *J. Am. Chem. Soc.* **1993**, *115*, 7884. (b) Hampden-Smith, M. J.; Ruegger, H. *Magn. Reson. Chem.* **1989**, *27*, 1107. (c) Azizian, H.; Dixon, K. R.; Eaborn, C.; Pidcock, A.; Shuaib, N.; Vinaixia, J. *J. Chem. Soc., Chem. Commun.* **1981**, 1020. (d) Butler, G.; Eaborn, C.; Pidcock, A. *J. Organomet. Chem.* **1979**, *181*, 47. (e) Watson, M.; Woodward, S.; Conole, G.; Kessler, M.; Sykara, G. *Polyhedron* **1994**, *13*, 2455.

trans-W(CO)₄(PR₃)(PR'₃),¹⁴ although this may not be definitive if a distorted *cis* geometry is present. The ³¹P{¹H} NMR spectra of the isostructural³ PiPr₃ complex W(CO)₃(PiPr₃)₂ showed some sign of temperature-dependent behavior, but it could not be resolved at any achievable low temperature, while [Re(CO)₃-(PiPr₃)₂]⁺ showed no spectral changes at all.^{7b} This would not be expected sterics should favor a *spyr* isomer for smaller *cis*-PiPr₃. Thus the increased bulkiness of the electronically-similar PCy₃ appears to be a critical factor (see below). Although the CO resonances could not be resolved in the ¹³C{¹H} NMR spectrum of Mo(CO)₃(PCy₃)₂ at -45 °C, the spectrum for [Re(CO)₃(PCy₃)₂]⁺ showed no evidence for geometric isomers.^{7b} Freezing out 5-coordinate isomeric structures by NMR is generally difficult in any event. Finally, the AB pattern has also been seen in the ³¹P NMR of 6-coordinate octahedral complexes by Caulton¹⁵ and Heinekey,^{7b} which in this case cannot be explained by a *spyr* isomer.

Heinekey and co-workers^{7b} offer a rationale for the AB signal in [Re(CO)₃(PCy₃)₂]⁺, where sterics (bulky PCy₃) are important. It directly relates to the report of Caulton¹⁵ concerning hindered rotation about the M–P bonds in 5- and 6-coordinate Ru and Ir systems containing bulky asymmetric *trans*-P-*t*-Bu₂Me phosphines. Steric interactions with the meridional ligands are proposed to lead to the existence of conformers with either no symmetry or mirror symmetry that result from freezing out the rotation about the M–P bond.¹⁵ Heinekey took this one step further and attributed the AB pattern in his Re system to a rotational conformer in which the bulky PCy₃ ligands are still *trans* yet inequivalent because of a staggered orientation of the cyclohexyl groups. The singlet signal is then proposed to be due to a eclipsed conformer in which the phosphines are related by a mirror plane of symmetry.



Both of these conformers (and no intermediate rotomers) have been seen in the X-ray crystal structures of these types of complexes. The structures of the agostic complexes for Cr, W, and Re are all staggered,^{2,3,7a} and those for their 6-coordinate adducts are generally eclipsed.^{1b,16–18} The W–ethylene complex (see below) has a staggered conformation, possibly because of steric pressure from the ethylene. The size of the meridional ligands is important in freezing out the conformers,¹⁵ and it was also suggested that the agostic interaction is a factor in increasing the barrier to rotation of the M–P bond in [Re(CO)₃(PCy₃)₂]⁺ (and presumably in M(CO)₃(PCy₃)₂ also).^{7b}

In summary, in the rationalization of the temperature-dependent behavior of the agostic complexes M(CO)₃(PCy₃)₂,

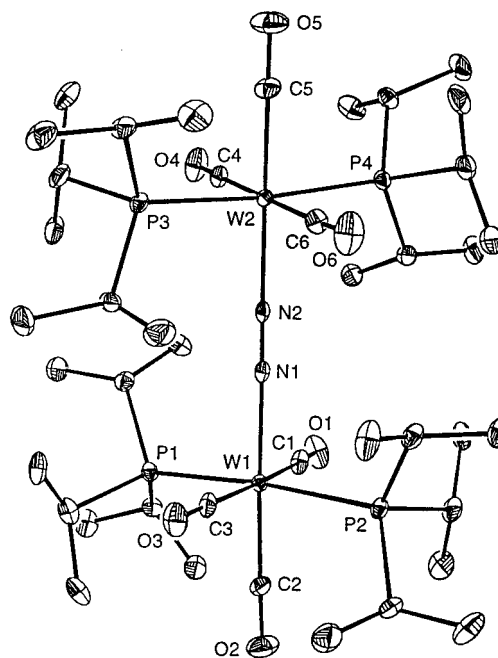


Figure 3. ORTEP diagram of [W(CO)₃(PiPr₃)₂]₂(μ-N₂) (**1**; 50% probability ellipsoids).

two scenarios are in principle consistent with most of the experimental results. An equilibrium between the highly fluxional agostic complex with *trans* phosphines and a minor *spyr* isomer containing inequivalent pseudo-*cis* phosphines is conceivable, but the existence of conformers resulting from hindered M–P rotation appears to be a better explanation.

Synthesis, Crystal Structure, and Reactivity of a Tungsten Dimer with a Bridging Dinitrogen Ligand. As mentioned above, the agostic C–H⋯M interaction in the M(CO)₃(PR₃)₂ complexes was easily displaced by a number of small molecules (Table 1). Early in the study of H₂ complexes, it was found^{1a,3} that the deep purple agostic complexes readily reacted with 1 atm of N₂ to form yellow Mo and W dinitrogen¹⁹ complexes. For M(CO)₃(PCy₃)₂, the products of these reactions were determined to be the terminal dinitrogen complexes M(CO)₃-(PCy₃)₂(N₂), largely based on the observation of NN stretching frequencies (Mo = 2159 cm⁻¹, W = 2120 cm⁻¹) in the infrared spectra of the solids.^{1a,3} In contrast, the IR spectra of the PiPr₃ congeners did not contain peaks that could be assigned to an NN stretch, and the complexes were orange rather than yellow. The Raman spectrum of the product of W(CO)₃(PiPr₃)₂ and N₂ was reported to contain bands at 1996 and 1939 cm⁻¹ that shifted to 1978 and 1896 cm⁻¹ on ¹⁵N₂ substitution. It was concluded that this is consistent with a dinuclear species with a bridging dinitrogen ligand wherein strong vibronic coupling exists between the NN stretch and a carbonyl stretch of the same symmetry.³ It is likely that the 1939 cm⁻¹ mode is assignable to ν(NN) because the calculated isotopic shift is 41 cm⁻¹ (for diatomic N₂), and the shift to 1896 cm⁻¹ would then be 43 cm⁻¹ (metal coordination and coupling to CO would affect the shift). The 1996 cm⁻¹ band would thus be due to a CO stretch mixed with ν(NN), shifting to 1978 cm⁻¹ for the ¹⁵N₂ isotopomer. The proposed structure, shown in eq 4, was recently confirmed in a

- (14) Schenk, W. A.; Buchner, W. *Inorg. Chim. Acta* **1983**, *70*, 189.
 (15) Notheis, J. U.; Heyn, R. H.; Caulton, K. G. *Inorg. Chim. Acta* **1995**, *229*, 187.
 (16) Heinekey, D. M.; Voges, M. H.; Barnhart, D. M. *J. Am. Chem. Soc.* **1996**, *118*, 10792.
 (17) Unpublished X-ray data for M(CO)₃(PCy₃)₂(H₂) for M = Mo and W (G. J. Kubas, P. J. Vergamini, H. J. Wasserman, and R. R. Ryan) and *trans*-W(CO)₄(PCy₃)₂ (L. S. Van Der Sluys, J. C. Huffman, and G. J. Kubas).
 (18) (a) Kubas, G. J.; Burns, C. J.; Khalsa, G. R. K.; Van Der Sluys, L. S.; Kiss, G.; Hoff, C. D. *Organometallics* **1992**, *11*, 3390. (b) Khalsa, G. R. K.; Kubas, G. J.; Unkefer, C. J.; Van Der Sluys, L. S.; Kubat-Martin, K. A. *J. Am. Chem. Soc.* **1990**, *112*, 3855.

- (19) Reviews on N₂ complexes: (a) Hidai, M.; Mizobe, Y. *Chem. Rev.* **1995**, *95*, 1115. (b) Pelikán, P.; Boca, R. *Coord. Chem. Rev.* **1984**, *55*, 55. (c) Chatt, J.; Dilworth, J. R.; Richards, R. L. *Chem. Rev.* **1978**, *78*, 589. (d) Chatt, J.; Leigh, G. J. *Chem. Soc. Rev.* **1972**, *1*, 121.

Table 2. Summary of Crystallographic Data

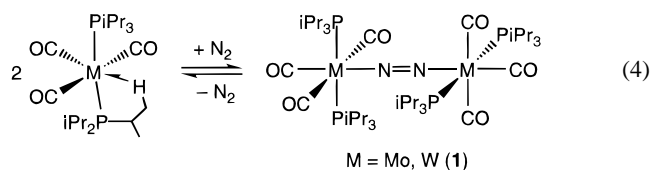
	1	2	5
empirical formula	C ₄₉ H ₉₂ N ₂ O ₆ P ₄ W ₂	C ₄₁ H ₇₀ O ₃ P ₂ W	C ₄₈ H ₆₄ O ₆ P ₂ Si ₂ W ₂
<i>a</i> , Å	13.676(3)	11.250(5)	15.760(2)
<i>b</i> , Å	13.833(2)	12.716(6)	17.427(2)
<i>c</i> , Å	16.447(4)	14.458(6)	17.957(2)
α , deg	70.80(2)	87.01(4)	
β , deg	84.90(2)	81.03(3)	90.390(8)
γ , deg	71.64(2)	74.04(3)	
<i>V</i> , Å ³	2788.4(10)	1964(2)	4931.8(10)
<i>Z</i>	2	2	4
<i>fw</i>	1296.8	856.8	1222.8
space group	<i>P</i> $\bar{1}$ (No. 2)	<i>P</i> $\bar{1}$ (No. 2)	<i>C</i> 2/ <i>c</i> (No. 15)
<i>T</i> , °C	–100	–70	–80
λ , Å	0.710 73	0.710 73	0.710 73
ρ_{calcd} , g cm ^{–3}	1.54	1.45	1.65
μ , cm ^{–1}	42.8	30.6	48.2
<i>R</i> ^a	0.030	0.029	0.061
<i>R</i> _w ^b	0.079	0.061	0.166

^a $R = \sum ||F_o| - |F_c|| / \sum |F_o|$, based on $F_o^2 > 2\sigma(F_o^2)$. ^b $R_w = [\sum [w(F_o^2 - F_c^2)^2] / \sum w(F_o^2)^2]^{1/2}$.

Table 3. Selected Bond Distances (Å) and Bond Angles (deg) for [W(CO)₃(PiPr₃)₂]₂(μ -N₂) (1)

W(1)–P(1)	2.5039(14)	W(2)–N(2)	2.121(4)
W(1)–P(2)	2.5152(14)	W(2)–P(3)	2.5255(14)
W(1)–C(1)	2.019(5)	W(2)–P(4)	2.5111(14)
W(1)–C(2)	1.965(5)	W(2)–C(4)	2.018(5)
W(1)–C(3)	2.027(5)	W(2)–C(5)	1.968(5)
W(1)–N(1)	2.117(4)	W(2)–C(6)	2.007(5)
N(1)–N(2)	1.136(6)		
P(1)–W(1)–N(1)	93.70(11)	N(2)–W(2)–C(5)	178.1(2)
P(2)–W(1)–N(1)	92.46(11)	N(2)–W(2)–C(6)	88.0(2)
P(3)–W(2)–N(2)	92.39(10)	W(1)–N(1)–N(2)	177.1(4)
P(4)–W(2)–N(2)	93.84(10)	W(2)–N(2)–N(1)	178.3(4)
N(1)–W(1)–C(1)	92.1(2)	P(1)–W(1)–P(2)	173.56(4)
N(1)–W(1)–C(2)	175.7(2)	P(3)–W(2)–P(4)	173.39(4)
N(1)–W(1)–C(3)	87.8(2)	C(1)–W(1)–C(3)	176.1(2)
N(2)–W(2)–C(4)	92.0(2)	C(4)–W(2)–C(6)	179.4(2)

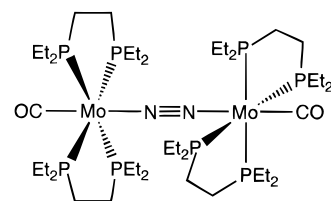
single-crystal X-ray crystallographic study performed on [W(CO)₃(PiPr₃)₂]₂(μ -N₂) (1). An ORTEP diagram is shown in Figure 3,



and crystal and data collection parameters as well as selected bond lengths and bond angles can be found in Tables 2 and 3, respectively. Both tungsten centers of **1** exist in an octahedral ligand environment with *trans* phosphines. When viewed down the W–N≡N–W axis, the corresponding ligands on each metal are staggered with respect to each other (L–M–M–L torsional angles are 54° on average). This staggering angle is similar to those in [RhH(PiPr₃)₂]₂(μ -N₂)²⁰ (55°) and [Mo(CO)(depe)₂]₂(μ -N₂)²¹ (~45° on average; depe = Et₂PC₂H₄PEt₂). From electronic arguments, this angle should be around 90° so that orthogonal π systems can be used by each metal for M→N back-bonding.^{19b,d} Offsetting steric effects usually come into play in bulky phosphine systems, and 45° staggering clearly reduces repulsion between the eight sets of phosphine organo groups in the Mo complex.

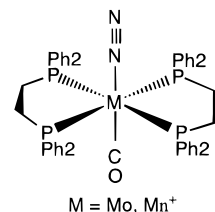
(20) Yoshida, T.; Okano, T.; Thorn, D. L.; Tulip, T. H.; Otsuka, S.; Ibers, J. A. *J. Organomet. Chem.* **1979**, *181*, 183.

(21) Luo, X. L.; Kubas, G. J.; Burns, C. J.; Butcher, R. J.; Bryan, J. C. *Inorg. Chem.* **1995**, *34*, 6538.



However, it would seem that the phosphine *iPr* groups would be further away from each other in the W and Rh complexes if the angle was in fact 90° as pictured in eq 4. The potential surface for twisting about the M–N≡N–M axis is likely to be very soft however, and the torsional angle could be established by optimal inter- as well as intramolecular packing of the *iPr* groups, as noted previously.²⁰ Steric repulsion between phosphines on neighboring metal centers is significantly greater in the PCy₃-substituted complex, and only the terminal complex W(CO)₃(PCy₃)₂(N₂) was observed. The structure of **1** is similar to that proposed for [W(CO)₃(PiPr₃)₂]₂(μ -pyrazine), the synthesis and electrochemistry of which were recently reported.²²

The N–N distance in [W(CO)₃(PiPr₃)₂]₂(μ -N₂) (1) of 1.136(6) Å represents only minimal lengthening of the N–N bond distance found in gaseous N₂ (1.0976 Å).²³ Interestingly, the N–N bond length is quite a bit shorter than that for other structurally-characterized W complexes with a bridging N₂ ligand, indicating less N₂ activation. For example, the N–N bond lengths in [Cl₂W(C₂Ph₂)(dme)₂]₂(μ -N₂),^{24a} [Cp*WMe₃]₂(μ -N₂),^{24b} [Cp*WMe₂(C₆F₅O)]₂(μ -N₂),²⁵ and [Cp*WMe₂(Smes)]₂(μ -N₂)²⁵ have been reported to be 1.292(16), 1.334(26), 1.26(2), and 1.27(2) Å, respectively.²⁶ Only in [Cl₂W(NPh)(PMe₃)₂]₂(μ -N₂) was the N–N bond length (1.19(2) Å) comparable to that found in **1**.²⁷ Interestingly, each of these compounds contained tungsten centers in high oxidation states compared to **1**, in which the metal center is formally W(0). A more electron rich tungsten center should result in a more activated dinitrogen ligand due to a greater degree of W→N back-bonding,^{19b,d} although this is clearly not the case with **1**. The structures of the above high-oxidation-state compounds suggest that they are most accurately described as tungsten hydrazido-(4–) complexes with a significant contribution from the W≡N–N≡W resonance structure.²⁵ In contrast, our structural studies would suggest that the most important resonance structure of **1** is W–N≡N–W. This situation is also present in [Mo(CO)(depe)₂]₂(μ -N₂), where the N–N bond length is 1.127(5) Å.²¹ The congeners with phenyl²⁸ (dppe) or benzyl^{8j} instead of ethyl substituents and also the cationic Mn analogue^{29a} [Mn(CO)(N₂)(dppe)₂]⁺ bind N₂ terminally.



It is difficult to sort out whether formation of terminal versus bridged solid-state structures is a consequence of more elec-

(22) Bruns, W.; Kaim, W.; Waldhör, E.; Krejčík, M. *Inorg. Chem.* **1995**, *34*, 663.

(23) Wilkinson, P. G.; Houk, N. B. *J. Chem. Phys.* **1956**, *24*, 528.

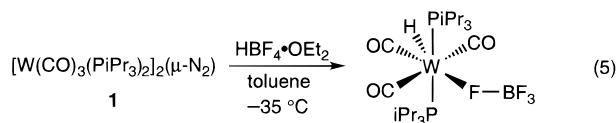
(24) (a) Churchill, M. R.; Li, Y.-J.; Theopold, K. H.; Schrock, R. R. *Inorg. Chem.* **1984**, *23*, 4472. (b) Churchill, M. R.; Li, Y.-J. *J. Organomet. Chem.* **1986**, *301*, 49.

(25) Regan, M. B.; Liu, A. H.; Finch, W. C.; Schrock, R. R.; Davis, W. M. *J. Am. Chem. Soc.* **1990**, *112*, 4331.

trophilic metal centers, steric congestion, stoichiometry, or differential solubilities. Indeed the terminal N_2 form³⁰ of $Mo(CO)(N_2)(depe)_2$ actually can be isolated in the presence of excess N_2 whereas the μ - N_2 -bridged complex was generated in a deficiency of nitrogen. Complex **1** precipitated even with excess N_2 present and was not very soluble. In solution, ^{15}N NMR on ^{15}N -enriched complexes is necessary to distinguish between terminal and bridging forms for these species. The Mn complex was found to contain only terminal N_2 in solution.^{29a}

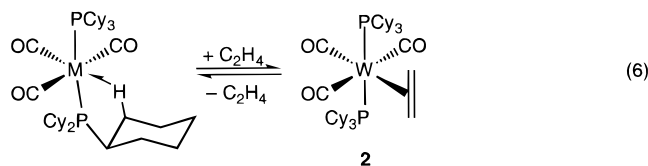
Consistent with the observation of a short N–N distance, the μ - N_2 ligand in **1** as well as that in the above Mo complex was somewhat labile. Although toluene solutions required heating to 100 °C under partial vacuum (or reflux in xylene under argon for the Mo system) to remove N_2 and regenerate the agostic complex, reactions in general proceeded through N_2 ligand loss. For example, the N_2 ligand of **1** was displaced at room temperature by a small excess of acetonitrile or under 1 atm of ethylene to form the 6-coordinate complexes $W(CO)_3(PiPr_3)_2(L)$ ($L = MeCN, C_2H_4$). Complex **1** was stable, however, in the presence of 12 equiv of THF in benzene. As a measure of ligand strengths in these systems, the order of enthalpy of binding toward $W(CO)_3(PCy_3)_2$ has been determined to be $THF < H_2 < N_2 < MeCN$ (~2–3 kcal/mol differentials).^{6b} The terminal N_2 ligand of $W(CO)_3(PCy_3)_2(N_2)$ was much more labile than the bridging N_2 in **1**.^{3,6a–c} A yellow toluene solution of the former quickly became purple when subjected to a vacuum at room temperature, indicating loss of N_2 and formation of the agostic complex. The terminal N_2 ligand was also labile in the solid state under vacuum. Similar observations were made with the ethylene complex $W(CO)_3(PCy_3)_2(\eta^2-C_2H_4)$ (see below) and the previously reported dihydrogen compound $W(CO)_3(PCy_3)_2(\eta^2-H_2)$.¹

Many examples of NH_3 or NH_2NH_2 formation from the reaction of mono- or multinuclear N_2 complexes with acids have been reported.^{19a,c} However, the reaction of **1** with 3.5 equiv of $HBF_4 \cdot OEt_2$ led to N_2 loss and formation of $W(CO)_3(PiPr_3)_2(H)(BF_4)$ as shown in eq 5. This 7-coordinate complex was



isolated as a solid by reacting $W(CO)_3(PiPr_3)_2$ with $HBF_4 \cdot OEt_2$ in toluene and was identified by comparison with the known $W(CO)_3(PCy_3)_2(H)(BF_4)$.³¹

Synthesis and NMR of $W(CO)_3(PCy_3)_2(\eta^2-C_2H_4)$, **2.** It has been known for some time that ethylene displaces the agostic interaction in $W(CO)_3(PCy_3)_2$ (eq 6, Table 1).^{1a,3} The properties of solid **2** that precipitates from toluene solution in eq 6 were very similar to those of $W(CO)_3(PCy_3)_2(\eta^2-H_2)$ and $W(CO)_3-$



$(PCy_3)_2(N_2)$, including color (yellow), solubility (low), and reversible binding of L. Toluene solutions of each complex rapidly became purple under reduced pressure at room temperature, indicating loss of L and re-formation of the agostic complex, and discoloration occurred in the solid state. The yellow color was immediately restored upon placing the complexes back under ethylene, dihydrogen, or dinitrogen. The properties of **2** in solution had not been previously studied, however, and NMR characterization (1H , ^{31}P , ^{13}C) of **2** is reported here (see Experimental Section). The NMR is consistent with complete ethylene ligation on addition of 1 atm of ethylene to $W(CO)_3(PCy_3)_2$.

The metal– H_2 σ -bond interaction in dihydrogen complexes has been considered to be directly analogous to metal–alkene π -bonding on the basis of theoretical calculations.^{32,33} The structure of $W(CO)_3(PiPr_3)_2(\eta^2-H_2)$ showed that the side-on bonded H_2 ligand is oriented parallel to the P–M–P axis rather than the OC–M–CO axis presumably to maximize metal $d\pi$ to H_2 σ^* back-bonding.^{1b–d} An alkene such as ethylene would be expected to maximize back-bonding to its π^* orbital similarly by aligning along the metal d orbitals of higher energy involved with the electron-donating phosphines. We were thus specifically interested in whether or not the ethylene ligand of **2** would be oriented in the same fashion as H_2 . The structure was also of interest because the steric constraints imposed by the bulky tricyclohexylphosphine groups could prevent this electronically favored orientation for the larger ethylene ligand. Propylene in fact did not form a stable complex (Table 1), presumably because steric factors would disallow this orientation (although it could conceivably fit along the OC–M–CO axis). Similarly, CO_2 did not bind to $W(CO)_3(PCy_3)_2$, although it is not clear whether the reasons for this are electronic, steric, or both. In the X-ray structure of $Mo(CO)_3(PiPr_3)_2(SO_2)$, the SO_2 ligand is η^1 -S-bound with a planar MSO_2 unit perpendicular to the P–Mo–P plane in order to align the $2b_1$ acceptor orbital of SO_2 for π back-bonding.³⁴ It was therefore thought that the structure determination of an η^2 π -ligand complex such as **2** would be revealing.

X-ray Crystal Structure of $W(CO)_3(PCy_3)_2(\eta^2-C_2H_4)$. An ORTEP diagram of **2** is shown in Figure 4. Table 2 contains crystal and data collection parameters, and selected bond lengths and bond angles can be found in Table 4. The most significant aspect of the structure of **2** is that it shows unambiguously that ethylene is bound to W in the same orientation as H_2 is bound in $W(CO)_3(PiPr_3)_2(\eta^2-H_2)$. This is expected from electronic considerations (more favorable back-bonding to π^* and σ^*

(26) The X-ray structure of $[W(N_2)_2(PEt_2Ph)_3]_2(\mu-N_2)$ has been reported; however, the state of the structure refinement did not allow discussion of bond distances: Anderson, S. N.; Richards, R. L.; Hughes, D. L. *J. Chem. Soc., Chem. Commun.* **1982**, 1291.

(27) Harlan, C. J.; Jones, R. A.; Koschmieder, S. U.; Nunn, C. M. *Polyhedron* **1990**, *9*, 669.

(28) Sato, M.; Tatsumi, T.; Kodama, T.; Hidai, M.; Uchida, T.; Uchida, Y. *J. Am. Chem. Soc.* **1978**, *100*, 4447.

(29) (a) King, W. A.; Luo, X.-L.; Scott, B. L.; Kubas, G. J.; Zilm, K. J. *Am. Chem. Soc.* **1996**, *118*, 6782. (b) King, W. A.; Kubas, G. J. To be published.

(30) Kubas, G. J.; Burns, C. J.; Eckert, J.; Johnson, S.; Larson, A. C.; Vergamini, P. J.; Unkefer, C. J.; Khalsa, G. R. K.; Jackson, S. A.; Eisenstein, O. *J. Am. Chem. Soc.* **1993**, *115*, 569.

(31) Van Der Sluys, L. S.; Kubat-Martin, K. A.; Kubas, G. J.; Caulton, K. G. *Inorg. Chem.* **1991**, *30*, 306.

(32) (a) Saillard, J.-Y.; Hoffmann, R. *J. Am. Chem. Soc.* **1984**, *106*, 2006.

(b) Burdett, K. J.; Eisenstein, O.; Jackson, S. A. In *Transition Metal Hydrides*; Dedieu, A., Ed.; VCH Publishers, Inc.: New York, 1992; pp 149–184 and references therein. (c) Lin, Z.; Hall, M. B. *Coord. Chem. Rev.* **1994**, *135/136*, 845.

(33) (a) Jean, Y.; Eisenstein, O.; Volatron, F.; Maoche, B.; Sefta, F. *J. Am. Chem. Soc.* **1986**, *108*, 6587. (b) Hay, P. J. *J. Am. Chem. Soc.* **1987**, *109*, 705. (c) Eckert, J.; Kubas, G. J.; Hall, J. H.; Hay, P. J.; Boyle, C. M. *J. Am. Chem. Soc.* **1990**, *112*, 2324. (d) Craw, J. S.; Bacskaý, G. B.; Hush, N. S. *J. Am. Chem. Soc.* **1994**, *116*, 5937. (e) Dapprich, S.; Frenking, G. *Organometallics* **1996**, *15*, 4547.

(34) Kubas, G. J.; Jarvinen, G. D.; Ryan, R. R. *J. Am. Chem. Soc.* **1983**, *105*, 1883.

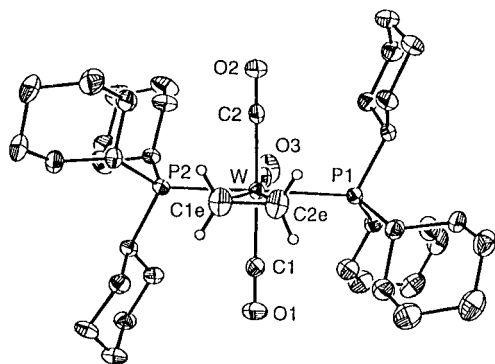


Figure 4. ORTEP diagram of $W(CO)_3(PCy_3)_2(C_2H_4)$ (**2**; 50% probability ellipsoids).

Table 4. Selected Bond Distances (Å) and Bond Angles (deg) for $W(CO)_3(PiPr_3)_2(\eta^2-C_2H_4)$ (**2**)

W–P(1)	2.5524(13)	W–C(2e)	2.339(4)
W–P(2)	2.5579(14)	C(1e)–C(2e)	1.378(6)
W–C(1)	2.007(4)	C(1)–O(1)	1.158(5)
W–C(2)	2.012(4)	C(2)–O(2)	1.157(5)
W–C(3)	1.977(4)	C(3)–O(3)	1.159(5)
W–C(1e)	2.338(4)		
P(1)–W–P(2)	165.26(3)	C(1e)–W–C(2e)	34.3(2)
P(1)–W–C(1)	87.88(12)	C(1)–W–C(1e)	86.9(2)
P(1)–W–C(2)	93.35(11)	C(1)–W–C(2e)	86.3(2)
P(1)–W–C(3)	81.42(12)	C(3)–W–C(1e)	163.36(15)
C(1)–W–C(2)	174.2(2)	C(3)–W–C(2e)	161.83(15)
C(1)–W–C(3)	96.6(2)		

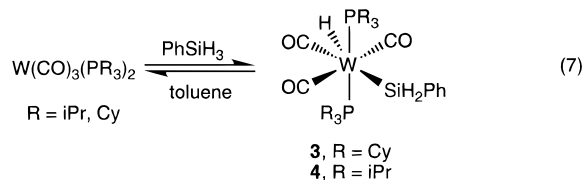
orbitals is available along the P–W–P axis) and reflects the similarity of metal–dihydrogen bonding to metal–olefin bonding. From a steric standpoint, it seemed somewhat surprising that this orientation is adopted. The hydrogens on ethylene were located and, despite their close proximity to the bulky phosphine ligands, appear to be in typical positions on the carbons (average C=C–H bond angle is 118°). Thus, electronic effects are clearly dominant here, and on going to propylene or C_2F_4 , steric effects (e.g., fluorine lone-pair repulsion) apparently prevent binding by disallowing orientation along P–W–P. It is interesting that the larger olefins do not give stable complexes (Table 1) when forced to orient along the OC–W–CO axis or off-axis (both of which should be sterically allowed but very unfavorable for back-bonding). This graphically illustrates just how critical back-bonding is in stabilizing olefin coordination, as is the case for H_2 , which can always orient to receive maximum back-donation because of its small size.

The ethylene C=C distance of 1.378(6) Å is at the lower limit of what is normally observed in ethylene complexes of tungsten, which typically range from about 1.38 to 1.45 Å.³⁵ This C=C distance in **2** represents only moderate elongation compared to that in free ethylene (1.337(2) Å).³⁶ Accordingly, the W–C distances of 2.338(4) and 2.339(4) Å are substantially longer than normally observed in $W(\eta^2-C_2H_4)$ complexes³⁵ although distances in this range have been observed previously.^{35f} The average W–P distance of 2.555 Å is the longest in a series

of structurally characterized $W(CO)_3(PCy_3)_2(L)$ compounds. For example, an average W–P bond length of 2.51 Å was found where $L = H_2$ or CO .¹⁷ In the agostic complex $W(CO)_3(PCy_3)_2$, the W–P distance of the phosphine without the C–H \cdots W interaction was 2.494(1) Å.³ Thus, overall it appears that the coordination sphere around the metal center in **2** is expanded slightly to accommodate the sterically less favored ethylene orientation. This was presumably counterbalanced by the gain in back-bonding here as opposed to the scenario where the ethylene lies off-axis or along the OC–W–CO axis.

Reactions of the Tungsten Agostic Complexes with Silanes.

Silanes, like H_2 , can bind to transition metal centers as σ -bond ligands in an η^2 -fashion.^{1g,37} Because of the close relationship between these ligands (η^2-H_2 and η^2-HSiR_3), we recently became interested in the reactivity toward silanes³⁸ of a range of Mo and W agostic complexes that form stable η^2-H_2 compounds. While $W(CO)_3(PR_3)_2$ ($R = iPr, Cy$) reacted in solution with H_2 to form an equilibrium mixture of the classical dihydride complex and the η^2-H_2 species, only the oxidative addition products were observed when these W complexes were treated with 1 equiv of $PhSiH_3$ (eq 7). Whereas the resonances



of the Si-bound hydrogens of free $PhSiH_3$ appeared in the 1H NMR spectrum in C_6D_6 at 4.23 ppm (25 °C, $J_{SiH} = 200.0$ Hz), the Si–H resonance of $W(H)(CO)_3(PCy_3)_2(SiH_2Ph)$ (**3**) at -45 °C in toluene- d_8 was found shifted downfield at 5.79 ppm, with smaller SiH coupling (176.8 Hz) as is typically observed in metal-bound silyl.^{1g} The W–H signal appeared at -4.51 ppm (t, $J_{HP} = 14.9$ Hz). The strongest evidence for the assignment of **3** as a 7-coordinate hydrido–silyl species rather than a 6-coordinate $\eta^2-H-SiH_2Ph$ species is the fact that the W–H resonance in the $^1H\{^{31}P\}$ NMR spectrum contained no Si satellites but did reveal $J_{WH} = 28.2$ Hz. The 1H and $^{31}P\{^1H\}$ NMR resonances for **3** broadened on warming to 0 °C, which is attributed to exchange across the equilibrium shown in eq 7. Broadening on cooling below -45 °C is most likely due to the slow exchange regime being approached for the intramolecular ligand rearrangement in the 7-coordinate compound (still unresolved at -80 °C). Similar observations were made for the analogous $PiPr_3$ compound **4** with the added feature that small coupling was observed between the W–H and the silicon-bound hydrogens ($J_{HH} = 1.8$ Hz). The spectroscopic changes observed in these reaction mixtures on warming were accompanied by a reversible color change from bright yellow at -45 °C to brown at room temperature. Both **3** and **4** decomposed to several products on standing at room temperature in solution. Unlike the tungsten complex, $Cr(CO)_3(PCy_3)_2$ did not react with silanes.

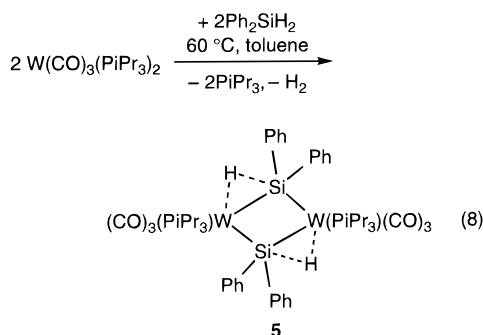
(35) (a) Radius, U.; Sundermeyer, J.; Pritzkow, H. *Chem. Ber.* **1994**, *127*, 1827. (b) Clark, G. R.; Nielson, A. J.; Rickard, C. E. F. *Acta Crystallogr.* **1993**, *C49*, 2074. (c) Aoshima, T.; Tamura, T.; Mizobe, Y.; Hidai, M. *J. Organomet. Chem.* **1992**, *435*, 85. (d) Chacon, S. T.; Chisholm, M. H.; Eisenstein, O.; Huffman, J. C. *J. Am. Chem. Soc.* **1992**, *114*, 8497. (e) Grevels, F.-W.; Jacke, J.; Betz, P.; Krüger, C.; Tsay, Y.-H. *Organometallics* **1989**, *8*, 293. (f) Alvarez, C.; Pacreau, A.; Parlier, A.; Rudler, H. *Organometallics* **1987**, *6*, 1057. (g) Carmona, E.; Galindo, A.; Poveda, M. L.; Rogers, R. D. *Inorg. Chem.* **1985**, *24*, 4033. (h) Sharp, P. R. *Organometallics* **1984**, *3*, 1217.

(36) Bartell, L. S.; Roth, E. A.; Hollowell, C. D.; Kuchitzu, K.; Young, J. E. *J. Chem. Phys.* **1965**, *42*, 2683.

(37) (a) Schubert, U. *Adv. Organomet. Chem.* **1990**, *30*, 151. (b) Schubert, U. In *Advances in Organosilicon Chemistry*; Marciniak, B., Chojnowski, J., Eds.; Gordon and Breach: Yverdon-les-Bains, Switzerland, 1994. (c) Lichtenberger, D. L.; Rai-Chaudhuri, A. *J. Am. Chem. Soc.* **1990**, *112*, 2492. (d) Corey, J. Y.; Braddock-Wilking, J. *MGCN, Main Group Chem. News* **1996**, *4*, 6. (e) Zhang, S.; Dobson, G. R.; Brown, T. L. *J. Am. Chem. Soc.* **1991**, *113*, 6908.

(38) (a) Luo, X.-L.; Kubas, G. J.; Burns, C. J.; Bryan, J. C.; Unkefer, C. J. *J. Am. Chem. Soc.* **1995**, *117*, 1159. (b) Luo, X.-L.; Kubas, G. J.; Bryan, J. C.; Burns, C. J.; Unkefer, C. J. *J. Am. Chem. Soc.* **1994**, *116*, 10312. (c) Luo, X.-L.; Kubas, G. J.; Burns, C. J. Unpublished results.

The low-temperature ^1H , $^1\text{H}\{^{31}\text{P}\}$, and $^{31}\text{P}\{^1\text{H}\}$ NMR spectra of $\text{W}(\text{CO})_3(\text{PiPr}_3)_2$ in the presence of Ph_2SiH_2 in toluene- d_8 indicated the presence of a mixture of compounds which could not be resolved (inconsistent with the presence of either the mononuclear oxidative-addition product or the $\eta^2\text{-H-SiHPh}_2$ product). The complex $\text{W}(\text{CO})_3(\text{PiPr}_3)_2$ did, however, react cleanly with an excess of Ph_2SiH_2 at 60°C in toluene to form the bridging silyl complex **5** shown in eq 8, which was isolated



as an orange crystalline solid in 34% yield. This reaction most likely began with the oxidative addition of Ph_2SiH_2 such as observed with PhSiH_3 , although no intermediates were observed and it is not clear at what point dimerization and H_2 loss occurred. The dimeric silane-bridged structure, confirmed by X-ray crystallography, is part of a growing class of complexes of this type containing bridging agostic Si-H interactions.³⁹ The ^1H NMR spectrum of **5** in $\text{THF-}d_8$ contained no resonances in the expected range for a terminal Si-H group but did contain a multiplet at -7.26 ppm which collapsed to a singlet in the $^1\text{H}\{^{31}\text{P}\}$ NMR spectrum. Interestingly, this resonance in the metal-hydride region had two sets of satellites of equal intensity ($J_{\text{WH}} = 42.4$ and 36.7 Hz). A three-center $\text{W}\cdots\text{Si}\cdots\text{H}$ interaction is suggested on the basis of the ^{29}Si NMR spectrum of **5** in $\text{THF-}d_8$, which contained only a broad doublet at 146.3 ppm ($\nu_{1/2} = 23$ Hz) with $J_{\text{SiH}} = 52$ Hz. The latter coupling constant is much lower than the Si-H coupling constant of 199.0 Hz for free Ph_2SiH_2 . The fact that the resonance collapsed to a singlet in the $^{29}\text{Si}\{^1\text{H}\}$ NMR spectrum confirmed that the coupling observed was indeed that of Si-H . This J_{SiH} is typical of J values for $\eta^2\text{-HSiR}_3$ compounds, which usually fall in the range $35\text{--}70$ Hz.^{37,38} The large upfield chemical shift of the W-H resonance suggests that the $\text{Si}\cdots\text{H}$ bond may have significant tungsten-hydride character and possibly a "stretched" $\text{Si}\cdots\text{H}$ bond distance analogous to stretched $\text{H}\cdots\text{H}$ distances over 1 Å in H_2 complexes.^{1g} A well-defined species with such a $\text{M-H}\cdots\text{Si}$ bonding description was only recently reported for a complex quite similar to **5**, $[\text{Fe}(\text{CO})_3(\mu\text{-SiHPh}_2)]_2$, which has a very long $\text{Si}\cdots\text{H}$ distance of 2.10 Å (50% longer than that (1.43 Å) in the nonbonded Si-H in the Ph_2SiH ligand).^{39f} The value of J_{SiH} , 24.3 Hz, is the lowest reported for a $\text{M}\cdots\text{H}\cdots\text{Si}$ interaction and is much lower than that for **5**. In light of this and the absence of structural location of hydrogen (see below), an unambiguous distinction between the $\text{M-H}\cdots\text{Si}$ interpretation and the conventional $\text{M}\cdots\text{H-Si}$ formalism cannot be made for **5**.

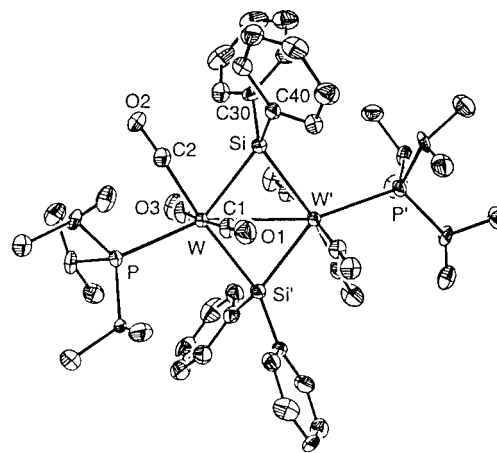


Figure 5. ORTEP diagram of $[\text{W}(\text{CO})_3(\text{PiPr}_3)(\mu\text{-SiHPh}_2)]_2$ (**5**; 50% probability ellipsoids).

Table 5. Selected Bond Distances (Å) and Bond Angles (deg) for $[\text{W}(\text{CO})_3(\text{PiPr}_3)(\mu\text{-SiHPh}_2)]_2$ (**5**)

W-Si	2.523(3)	W-W'	3.2256(8)
W-Si'	2.708(3)	Si-C(30)	1.887(11)
W-P	2.528(3)	Si-C(40)	1.883(10)
W-C(1)	2.008(9)	C(1)-O(1)	1.158(12)
W-C(2)	1.984(11)	C(2)-O(2)	1.160(14)
W-C(3)	2.029(10)	C(3)-O(3)	1.119(13)
P-W-Si	146.47(9)	Si-W-C(3)	95.4(3)
P-W-Si'	108.92(8)	Si-W-Si'	103.96(7)
P-W-C(1)	89.0(3)	W-Si-W'	76.04(7)
P-W-C(2)	80.3(3)	C(30)-Si-C(40)	101.6(5)
P-W-W'	157.63(6)	C(1)-W-C(3)	175.6(4)
Si-W-C(1)	81.5(3)	C(2)-W-W'	122.1(3)
Si-W-C(2)	69.2(3)		

X-ray Crystal Structure of $[\text{W}(\text{CO})_3(\text{PiPr}_3)(\mu\text{-SiHPh}_2)]_2$, **5.** Structural studies on related dimeric compounds containing bridging $\text{SiH}_n\text{R}_{3-n}$ ($n = 1, 2$) ligands have suggested that, in a bonding arrangement such as shown in eq 8, one should expect a longer M-Si distance in the 3-center, 2-electron bond than in the normal M-Si bond.³⁹ For this reason and also in an attempt to find an elongated Si-H bond distance, we performed an X-ray crystallographic study on **5**. An ORTEP diagram of **5** is shown in Figure 5. Table 2 contains crystal and data collection parameters, and Table 5 gives selected bond lengths and bond angles.

The crystal structure of **5** confirmed that it is a dimeric species with bridging SiPh_2 groups. From the view provided in Figure 6 it can be seen that the four-membered ring is roughly coplanar with the P atom and the C(2)-O(2) carbonyl group. The W-W distance was found to be $3.2256(8)$ Å, consistent with the existence of a M-M bond as in the closely related complex $[\text{W}(\text{CO})_4(\mu\text{-SiHEt}_2)]_2$, where CO is present in place of PiPr_3 and $\text{W-W} = 3.183(1)$ Å.^{39e} Both tungsten centers in these dinuclear complexes have highly distorted octahedral coordination about them. Unfortunately, the hydrogens were not located, but as illustrated in Figure 7, the P atoms are pushed away from the Si atoms "cis" to them ($\text{P-W-Si} = 108.9^\circ$), indicating that the hydrogens presumably attached to the Si and W atoms are situated between P and Si in the plane of the four-membered ring. The strongest structural evidence that **5** contains two 3-center, 2-electron $\text{W}\cdots\text{H}\cdots\text{Si}$ interactions is the observation of two distinctly different W-Si bond distances ($2.523(3)$ and $2.708(3)$ Å), with the longer being *cis* to the position in which the hydride ligand is proposed to exist. Such bond length differences are always observed in bridging silane compounds in which there is a proposed $\text{W}\cdots\text{H}\cdots\text{Si}$ interaction as depicted in Figure 7. For example, $[\text{W}(\text{CO})_4(\mu\text{-SiHEt}_2)]_2$ had W-Si

(39) (a) Suzuki, H.; Takao, T.; Tanaka, M.; Moro-oka, Y. *J. Chem. Soc., Chem. Commun.* **1992**, 476. (b) Fryzuk, M. D.; Rosenberg, L.; Rettig, S. J. *Organometallics* **1991**, *10*, 2537. (c) Aitken, C. T.; Harrod, J. F.; Samuel, E. *J. Am. Chem. Soc.* **1986**, *108*, 4059. (d) Auburn, M.; Ciriano, M.; Howard, J. A. K.; Murray, M.; Pugh, N. J.; Spencer, J. L.; Stone, F. G. A.; Woodward, P. *J. Chem. Soc., Dalton Trans.* **1980**, 659. (e) Bennett, M. J.; Simpson, K. A. *J. Am. Chem. Soc.* **1971**, *93*, 7156. (f) Simons, R. S.; Tessier, C. A. *Organometallics* **1996**, *15*, 2604. (g) Takao, T.; Yoshida, S.; Suzuki, H.; Tanaka, M. *Organometallics* **1995**, *14*, 3855.

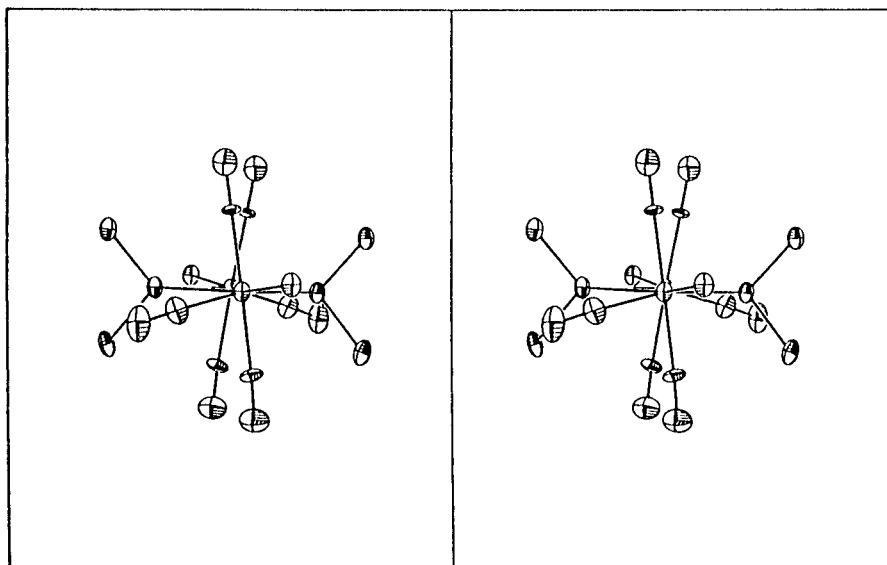


Figure 6. Stereoview of **5** as viewed down the W–W axis. The isopropyl groups and phenyl carbons other than the ipso carbons are omitted for the sake of clarity.

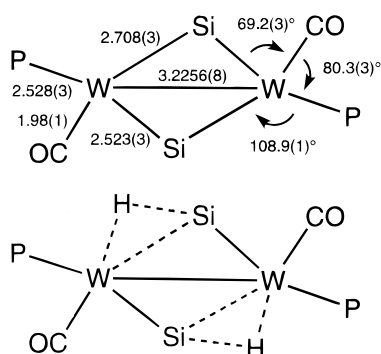


Figure 7. Drawing of **5** with the crystallographically determined bond lengths and angles in the plane of the four-membered ring. The lower figure shows probable positions of hydrogens.

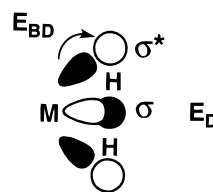
distances of 2.586(5) and 2.703(4) Å with the same overall geometry as found for **5**.^{39e} Unfortunately, no spectroscopic evidence for W···H···Si interaction was offered.

Comparisons of H–H versus Si–H σ -Bond Activation and Oxidative-Addition (OA) Processes. Much current effort is being focused on σ -bond activation,^{1g} and it would be quite informative to correlate well-studied H₂ bonding and activation with that for silanes, which could model alkane activation. Agostic complexes such as M(CO)₃(PR₃)₂ (M = Mo, W) and M(CO)(R₂PC₂H₄PR₂)₂ (M = Mo, Mn⁺)^{8j,21,28–30} generally react with silanes similarly to H₂, i.e. to form both OA products as well as M···H–Si σ -complexes. As yet, few metal fragments bind both silanes and H₂, especially near the point of OA. W(CO)₃(PR₃)₂ cleaves silanes yet binds H₂, which unexpectedly is opposite to the reactivity on Mo(CO)(Et₂PC₂H₄PEt₂)₂. The possible reasons for this will be discussed here.

For H₂ binding on a wide variety of metal–ligand fragments, a near continuum of H–H distances (0.85–1.5 Å) exists (cf. 0.74 Å in H₂).^{1e–h} This blurs the dihydrogen–dihydride formalism, i.e. the point at which the H–H bond can be considered to be fully broken (1.6 Å is often quoted). Maseras recently studied this theoretically by applying Bader's⁴⁰ atoms-

in-molecules formalism.⁴¹ Complexes with H···H separations >1.3 Å were best viewed as dihydride complexes with weak H···H interactions, while a separation of 0.82 Å corresponds to a true dihydrogen complex; i.e., a clear bond path connects the hydrogens. The value in W(CO)₃(PCy₃)₂(H₂) is 0.82 Å by neutron diffraction but is probably closer to 0.89 Å, the solid state NMR value.⁴² A distance near 1.0 Å represented an intermediate state of activation with some residual H–H bonding, and a similarly stretched Si–H bond (2.10 Å, which roughly corresponds to a 1.05 Å H–H distance) has now been identified.^{39f}

Back-bonding from M to the X–H σ^* orbital has widely been accepted to control the X–H distance (X = H, C, Si, etc.) along the reaction coordinate toward OA and confers stability to H₂ complexes; e.g., poor back-bonding fragments such as Cr(CO)₅ give thermally unstable H₂ complexes.⁵ However, highly electrophilic cationic centers such as [Re(CO)₃(PCy₃)₂]⁺ and [Mn(CO)(dppf)₂]⁺ can bind H₂ by increased σ donation to the metal, offsetting decreased back-bonding.^{7,29} σ donation alone cannot cause H–H bond rupture; back-bonding must complete this task. Sorting out these two components is important in understanding σ -bond activation. Recent theoretical studies by Ziegler on our group 6 complexes⁴³ and also group 8 systems⁴⁴ indicate that the back-donation component, E_{BD} , of the total M–H₂ orbital interaction energy can be quantified and separated from σ -donation E_D and is comparable to, or exceeds, the latter even when H–H distances are short (0.85–0.9 Å).



E_{BD} values as high as 21 kcal/mol were calculated, and

(40) (a) Bader, R. F. W. *Atoms in Molecules: a Quantum Theory*; Clarendon: New York, 1990. (b) Bader, R. F. W. *Acc. Chem. Res.* **1985**, *18*, 9.

(41) Maseras, F.; Lledos, A.; Costas, M.; Poblet, J. M. *Organometallics* **1996**, *15*, 2947.

(42) (a) Zilm, K. W.; Merrill, R. A.; Kummer, M. W.; Kubas, G. J. *J. Am. Chem. Soc.* **1986**, *108*, 7837. (b) Zilm, K. W.; Millar, J. M. *Adv. Magn. Opt. Reson.* **1990**, *15*, 163.

(43) Li, J.; Ziegler, T. *Organometallics* **1996**, *15*, 3844.

(44) Li, J.; Dickson, R. M.; Ziegler, T. *J. Am. Chem. Soc.* **1995**, *117*, 11482.

Table 6. Axial CO Stretching Frequencies (cm^{-1}) for Complexes Containing H_2 versus Other Ligands

L	$\text{W}(\text{CO})_5(\text{L})^a$	$\text{W}(\text{CO})_3(\text{PCy}_3)_2(\text{L})^b$	$\text{Mo}(\text{CO})(\text{dppe})_2(\text{L})^c$
SO_2	2002	1873	1901
H_2	1971	1843	1815
C_2H_4	1973	1834	1813
N_2	1961	1835	1809
argon	1932		
$\text{CH}_4/\text{agostic}^d$	1926	1797	1723
pyridine	1921	1757	1718
NR_3	1919 ^e	1788 ^f	1723 ^e

^a References 5d, 56 (SO_2), 57 (N_2). ^b References 1a, 3. ^c References 30 (SO_2 , H_2 , agostic), 58. ^d $\text{L} = \text{CH}_4$ (matrix) for $\text{W}(\text{CO})_5(\text{L})$; agostic C–H for others. ^e $\text{NR}_3 = \text{NEt}_2\text{H}$. ^f $\text{NR}_3 = \text{NH}_2\text{Bu}$.

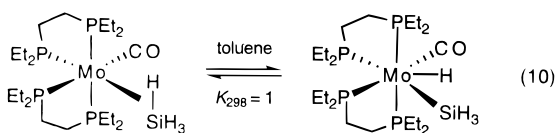
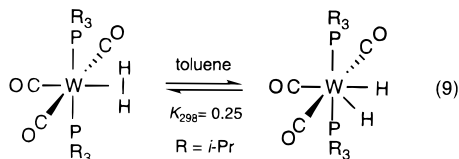
experimentally, H_2 rotational barriers as high as 11 kcal/mol have now been seen in H_2 complexes,⁴⁵ implying at least this much back-donation. Surprisingly, E_{BD} in $\text{Mo}(\text{CO})_5(\text{H}_2)$ is about half E_{D} despite the seemingly poor back-bonding ability of this fragment. These unexpected findings suggest that H_2 complexes might best be pictured as triangulo species with partial bonds joining the three atoms rather than the usual 3-center representation.



In line with this, our normal-coordinate vibrational analysis of $\text{W}(\text{CO})_3(\text{PCy}_3)_2(\text{H}_2)$ shows that the H–H and W–H stretches are highly coupled and that the force constants for these coordinates are *nearly equal*, with the H–H constant reduced 4-fold from its value in free H_2 .⁴⁶

Dihydrogen is an excellent π -acceptor, perhaps even superior to CO ⁴⁷ and at least comparable to olefins and N_2 judging by similarity of ν_{CO} for CO *trans* to $\text{L} = \text{H}_2$, N_2 , C_2H_4 in $\text{M}(\text{CO})_5\text{L}$ in liquid Xe ,^{5d} heptane,^{5j} and the gas phase^{5k} and also in $\text{W}(\text{CO})_3(\text{PR}_3)_2(\text{L})$ and $\text{Mo}(\text{CO})(\text{dppe})_2(\text{L})$ (Table 6). Strong acceptors (SO_2) give high ν_{CO} while pure σ -donors give much lower values; the values all drop proportionately as the electron richness of the metal center increases from left to right. Importantly, these data also show that CH_4 and agostic C–H are *poor* π -acceptors (similar to amines), which had been rationalized theoretically^{32a} by orbital mismatch (overlap is large between metal d and H_2 σ^*). This lack of back-bonding helps explain the instability of alkane complexes.⁵ⁱ

In contrast to “stretching” the X–H bond, some systems give *equilibria* between σ -complex and OA products (eqs 9 and 10).



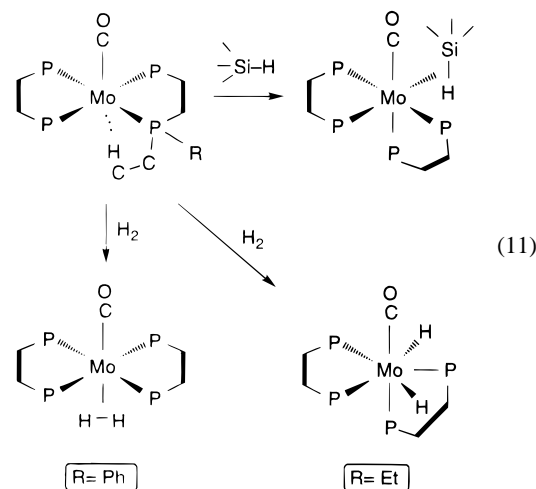
(45) Jalon, F. A.; Otero, A.; Manzano, B. R.; Villasenor, E.; Chaudret, B. *J. Am. Chem. Soc.* **1995**, *117*, 10123.

(46) Bender, B. R.; Kubas, G. J.; Jones, L. H.; Swanson, B. I.; Eckert, J.; Capps, K. B.; Hoff, C. D. *J. Am. Chem. Soc.*, in press.

(47) Morris, R. H.; Schlaf, M. *Inorg. Chem.* **1994**, *33*, 1725.

At least a dozen such equilibria have been observed for H_2 activation but only two for Si–H bond activation.^{38a,39g} Remarkably, ΔG^\ddagger for eq 9 (16.0 kcal/mol at 298 K)^{18b} is very similar to that for eq 10 (15.3 kcal/mol at 333 K),^{38c} indicating that H–H and Si–H cleavages have reasonably similar reaction coordinates. However, there are subtle differences in H–H and Si–H activations, as seen by the work here that shows silanes undergo complete OA on $\text{W}(\text{CO})_3(\text{PR}_3)_2$ whereas H_2 does so only in equilibrium fashion. It is instructive to examine Table 7 which compares activation of these ligands on various d^6 centers, along with other π -acceptor, “electronic gauge” ligands. The values of J_{HD} , J_{SiH} , and H–H distance correlate well as indicators of the activation of the σ bond, and ν_{NN} and ν_{SO} measure the metal’s electron richness (back-bonding ability). Morris proposed that M– H_2 binding is stable if ν_{NN} is 2060–2150 cm^{-1} ,⁴⁸ and this has held up fairly well (highly electrophilic centers may be an exception). Thus H_2 (and silane) binding to $\text{Cr}(\text{CO})_5$ is unstable ($\nu_{\text{NN}} = \sim 2230$ cm^{-1}) but H_2 cleaves on the much more electron-rich $\text{Mo}(\text{CO})(\text{depe})_2$ ($\nu_{\text{NN}} = 2050$ cm^{-1}).³⁰ However the H–H bond is never > 0.9 Å for any of the group 6 systems and breaks suddenly, whereas it usually elongates for later transition metals. The presence of a strong π -acceptor, CO , *trans* to H_2 is a major factor because it disfavors OA of H_2 .³³

In comparison to H_2 , PhSiH_3 did *not* oxidatively add to $\text{Mo}(\text{CO})(\text{depe})_2$ *even though silanes appear to be the better* π -acceptors because, unlike H_2 , silanes rearrange their coordination position to be *cis* to CO ,³⁸ *ostensibly to avoid competing with CO for back-donation*.



Theoretical calculations⁴⁹ on $\text{Mo}(\text{CO})(\text{PH}_3)_4(\text{H}\cdots\text{SiH}_3)$ also favored coordination of SiH_4 *cis* to CO for this electronic reason. The reversal of results for H_2 and PhSiH_3 addition to $\text{W}(\text{CO})_3(\text{PR}_3)_2$ compared to that for $\text{Mo}(\text{CO})(\text{depe})_2$ demonstrates that a fine balance of forces exists here that may go beyond electronics, e.g. steric factors or structural rearrangement barriers for 6- versus 7-coordination. Theoretical and experimental studies indicate overall bond energetics can be crucial.⁵⁰ The relative M–X energies can offset the X–H energy difference (H–H is 104 kcal/mol versus only 72–90 kcal/mol for Si–

(48) Morris, R. H.; Earl, K. A.; Luck, R. L.; Lazarowych, N. J.; Sella, A. *Inorg. Chem.* **1987**, *26*, 2674.

(49) Fan, M.-F.; Jia, G.; Lin, Z. *J. Am. Chem. Soc.* **1996**, *118*, 9915.

(50) (a) Musaev, D.; Morokuma, K. *J. Am. Chem. Soc.* **1995**, *117*, 799. (b) Maseras, F.; Lledos, A. *Organometallics* **1996**, *15*, 1218. (c) Esteruelas, M. A.; Oro, L. A.; Valero, C. *Organometallics* **1991**, *10*, 462. (d) Luo, X.-L.; Crabtree, R. H. *J. Am. Chem. Soc.* **1989**, *111*, 2527. (e) Poulton, J. T.; Sigala, M. P.; Eisenstein, O.; Caulton, K. G.

Table 7. Comparison of Small-Molecule Binding and Activation on Various d⁶ Metal Fragments (OA = Oxidative Addition)

metal fragment	H ₂		PhSiH ₃	Ph ₂ SiH ₂	N ₂	SO ₂
	<i>J</i> _{HD} ^a	H–H ^b	<i>J</i> _{SiH} ^c	<i>J</i> _{SiH} ^c	ν_{NN}^d	ν_{SO}^e
Cr(CO) ₃ (PR ₃) ₂	35 ^f	0.85 ^g	N.R. ^g		2128 ^g	
W(CO) ₃ (PR ₃) ₂	34, equil OA ^f	0.89 ^f	OA	eq 8	2120 ^g	1237 ^g
Mo(CO)(Ph ₂ PC ₂ H ₄ PPh ₂) ₂	34	0.88	57, weak	weak	2090	1209
Mo(CO)(Bz ₂ PC ₂ H ₄ PBz ₂) ₂	30	0.87	41		2062	1180
Mo(CO)(Et ₂ PC ₂ H ₄ PEt ₂) ₂	OA		39	50		2050
[Mn(CO)(Ph ₂ PC ₂ H ₄ PPh ₂) ₂] ⁺	33	0.89	weak ^h		2167	1164
CpMn(CO) ₂	33			~63.5 ⁱ	2173	1270
[CpFe(CO)(PEt ₃)] ⁺	31.6			58		~1282 ^j

^a Hz. References (from top down): 6d, 1c, 30, 8j, 29a, 59, 52. ^b Å. From solid state ¹H NMR (refs 6d, 41, 29a). ^c Hz. For coordinated Si–H bond (refs 38b, 37a, 52; values for uncoordinated Si–H = 164–205 Hz). ^d cm⁻¹. References 2, 3, 30, 8j, 29, 51. ^e cm⁻¹; asymmetric stretch (refs 8j (Mo), 60–62). ^f R = iPr. ^g R = Cy. ^h *J*_{SiH} could not be measured because of broadening due to the quadrupolar Mn nucleus. ⁱ Value for MeCp derivative. ^j Value for [CpFe(dppe)(SO₂)]⁺.

H^{50f}). Thus calculations by Maseras and Lledos^{50b} showed little energy difference between OsCl(CO)(PH₃)₂(H)(η^2 -H–SiH₃) and OsCl(CO)(PH₃)₂(SiH₃)(η^2 -H₂), although experimentally there is preference for the latter.^{50c} On the other hand, the [IrH₂(η^2 -HSiEt₃)₂(PPh₃)₂]⁺ structure was found on this fragment.^{50d} Addition of H₂ to RuH₂(CO)(PtBu₂Me)₂ gave the η^2 -H₂ adduct, but HSiMe₃ addition led to OA.^{50e} Thus the relative stability of the two forms may depend on a subtle balance of thermodynamics by themselves or in combination with back-bonding arguments.

It might be possible to conclude from Table 7 that silanes undergo OA more easily than H₂ as the electrophilicity of the metal center increases, perhaps because of the superior π -acceptor strength of Si–H. As the metal becomes more electron rich, the differences in π -acceptor strength of the σ -ligands should not matter as much in bond cleavage, and H₂ could even undergo OA more easily than silanes for steric or other reasons. The W(CO)₃P₂ center is more electrophilic than Mo(CO)P₄ on the basis of IR evidence in Tables 6 and 7 and calculations of *E*_{BD}⁴³ and indeed cleaves silanes more easily than H₂. However, unlike H–H activation, Si–H (and C–H) activation can be tuned two ways: varying the substituents at both M and Si. Making the Si more electropositive using substituents such as Cl favors back-bonding that increases binding energy and ultimately leads to Si–H cleavage.^{37a–d} Significantly, the opposite trend is seen^{37e} on highly electrophilic centers such as Cr(CO)₅, where *E*_D is more important to the binding energy. SiH₄ undergoes equilibrium OA on Mo(CO)(depe)₂ (eq 10), but organosilanes bind only as σ -ligands. As seen in Table 7, *J*_{SiH} is 11 Hz lower for the PhSiH₃ complex than the Ph₂SiH₂ complex, while the Si–H distance (1.77(6) Å^{38b}) is correspondingly longer than in the latter (1.60(6) Å^{38c}). Therefore comparisons of silane and H₂ activation are valid only for silanes with similar substituents. The most electrophilic fragment in Table 7, CpMn(CO)₂, readily coordinates Ph₂SiH₂ and oxidatively adds HSiCl₃³⁷ but was only recently found to give an isolable H₂ complex⁵¹ from supercritical CO₂ (*J*_{HD} = 33 Hz; i.e. relatively unactivated). Even more electrophilic CpV(CO)₃⁵² and [CpFe(CO)(PEt₃)]⁺⁵³ give unstable H₂ complexes but easily bind silanes and cleave⁵² HSiEtCl₂.

Unlike the above systems, Cr(CO)₃(PCy₃)₂ coordinates H₂ under several atmospheres of pressure in solution^{2,6d} but does

not interact with excess PhSiH₃ (steric congestion around a smaller first-row metal² may inhibit silane binding). As mentioned above, the highly electrophilic cationic [Mn(CO)(dppe)₂]⁺ containing a double agostic interaction^{29a} binds H₂ similarly to Mo(CO)(dppe)₂ because increased H₂ to Mn⁺ σ donation offsets decreased back-bonding. However, H₂ binds significantly more strongly than either PhSiH₃, SiH₄, or N₂ to Mn⁺ as compared to Mo.^{29b}

Theoretical comparison between Si–H and H–H σ -bond activation was recently made by Fan et al.,⁴⁹ by Bader-type analysis of the electron density around the Mo(H \cdots Si) triangle in Mo(CO)(PH₃)₄(H \cdots SiH₃). A generic conclusion was made that coordinated Si–H lies closer to the classical hydrido-silyl extreme but that “the H–H bond remains essentially unperturbed by M \rightarrow H₂ σ^* back-bonding, and it lies closer to the nonclassical dihydrogen extreme”. Regarding Si–H binding, this could well be the situation in many cases, particularly in [Fe(CO)₃(μ -SiHPh₂)₂], where Si \cdots H is 2.10 Å (50% elongation),^{39f} and perhaps even in Mo(CO)(depe)₂(PhSiH₃), where Si \cdots H is elongated 25%. However, for H₂ activation, the conclusions are too general since many complexes with elongated H \cdots H exist that clearly are perturbed by back-bonding. Also, all indications point to strong M–H₂ back-bonding even in true unstretched H₂ complexes and similarity in the reaction coordinate for OA of H–H and Si–H bonds. Inexplicably however, in some cases, particularly for group 6 complexes, the H–H bond does seem less perturbed by back-bonding than it should be. Why are H–H distances not longer than 0.9 Å in H₂ complexes perilously close to OA, such as Mo(CO)(dppe)₂(H₂) where *E*_{BD} is 21 kcal/mol, nearly twice that for *E*_D? Also, why do tautomeric equilibria occur between a σ complex with a short X–H and the OA product (eqs 9 and 10) instead of bond elongation?

A possible answer is that complexes with H–H distances of 0.85–0.95 Å and high *J*_{HD} values (>30 Hz) may actually lie further along the reaction coordinate than originally believed, which is supported by the H–H force constant⁴⁶ and *E*_{BD} data. Complexes with much longer H–H distances (“stretched H₂ complexes” or “compressed dihydrides”), would then lie even further along the reaction coordinate. H atom abstraction enthalpies calculated by Morris indeed suggest that complexes with H–H distance > 1.1 Å contain little H–H bonding and are more consistent with M–H bonding alone.^{1h} All of this is very subjective because of the continuum nature of the bond activation. Even classical dihydrides have been shown calculationally to have weak residual H \cdots H interactions,⁵⁴ and trying

Inorg. Chem. **1993**, *32*, 5490. (f) The value of 72 kcal/mol for the Si–H bond energy of SiH₄ in ref 50b is probably too low because it is an average value. The energy of the HSi₃–H bond is 90 kcal/mol according to: Walsh, R. *Acc. Chem. Res.* **1981**, *14*, 246.

(51) Banister, J. A.; Lee, P. D.; Poliakoff, M. *Organometallics* **1995**, *14*, 3876.

(52) George, M. W.; Haward, M. T.; Hamley, P. A.; Hughes, C.; Johnson, F. P. A.; Popov, V. K.; Poliakoff, M. *J. Am. Chem. Soc.* **1993**, *115*, 2286.

(53) Scharer, E.; Chang, S.; Brookhart, M. *Organometallics* **1995**, *14*, 5686.

(54) Jackson, S. A.; Eisenstein, O. *J. Am. Chem. Soc.* **1990**, *112*, 7203.

(55) (a) Lang, R. F.; Ju, T. D.; Kiss, G.; Hoff, C. D.; Bryan, J. C.; Kubas, G. J. *J. Am. Chem. Soc.* **1994**, *116*, 7917. (b) Lang, R. F.; Ju, T. D.; Kiss, G.; Hoff, C. D.; Bryan, J. C.; Kubas, G. J. Submitted to *Inorg. Chim. Acta*.

to place boundaries on categorizations such as "stretched dihydrogen complexes" or pinpoint the exact moment of H–H cleavage will always be debatable.

Summary and Conclusions

NMR investigation of the temperature-dependent behavior of the agostic species $M(\text{CO})_3(\text{PCy}_3)_2$ indicates the presence of conformational isomers resulting from hindered rotation of the M–P bond or, less likely, a geometric isomer with pseudo-*cis* PCy_3 ligands. The structure of $\text{W}(\text{CO})_3(\text{PCy}_3)_2(\text{C}_2\text{H}_4)$ demonstrates that, despite crowding by the large phosphines, ethylene has a strong preference for aligning along the P–W–P axis as in the case of H_2 coordination. Unlike the case of H_2 σ coordination, PhSiH_3 oxidatively adds to $\text{W}(\text{CO})_3(\text{PR}_3)_2$. On the other hand, Ph_2SiH_2 reacts at 60 °C to eliminate H_2 and PiPr_3 and form $[\text{W}(\text{CO})_3(\text{PiPr}_3)(\mu\text{-SiHPh}_2)]_2$ with 3-center $\text{W}\cdots\text{H}\cdots\text{Si}$ interactions.

Evidence indicates that both H_2 and silane ligands are powerful π -acceptors like ethylene. Activation of these σ ligands on metal fragments follows a relatively simple model yet offers a wealth of opportunity for study. There are at least five primary variables in $M(\eta^2\text{-X-H})$ systems influencing the electronics and hence activation toward OA: the nature of M and X, the substituents at both M and X, and overall charge. Additionally, steric factors and overall energetics of OA processes could play important roles in determining the point at which a σ bond breaks. Thus, despite the similarity of the reaction coordinate for H–H and Si–H bond cleavage, on some metal fragments, e.g. $\text{Mo}(\text{CO})(\text{depe})_2$, H_2 undergoes OA more easily than silanes, but on others such as $\text{W}(\text{CO})_3(\text{PR}_3)_2$, the reverse is true.

Correlations such as those in Table 7 should be valuable in defining electronic structure requirements for the optimal design of metal fragments for σ -bond activation. Indications are that metal–alkane complexes could best be stabilized toward isolation on extremely electrophilic, positively-charged metal centers, which were recently found to give quite stable silane and H_2 complexes. Since back-bonding is generally weak in alkane complexes, it might be more important to increase σ donation as much as possible (this also avoids C–H bond cleavage). Theoretical studies predict stronger stabilization of charged bare-metal $M^+-\text{CH}_4$ complexes compared to their neutral analogues,⁶³ and experimental studies show that CH_4 actually binds more strongly than H_2 to Co^+ .⁶⁴

Experimental Section

General Materials and Procedures. Unless otherwise noted, all reactions and manipulations were performed in dry glassware under a helium atmosphere in a Vacuum Atmospheres drybox or by using standard Schlenk techniques. All ^1H , $^1\text{H}\{^{31}\text{P}\}$, $^{13}\text{C}\{^1\text{H}\}$, and $^{31}\text{P}\{^1\text{H}\}$ NMR spectra were recorded on either a commercial 500 MHz Bruker AMX series spectrometer or a Bruker WM 300 MHz spectrometer.

All J values are reported in hertz. IR spectra were obtained on a Bio-Rad FTS-40 instrument. Elemental analyses were obtained from Oneida Research Services, Inc.

Toluene, hexane, Et_2O , and THF were distilled from sodium/benzophenone. The $M(\text{CO})_3(\text{PR}_3)_2$ ($M = \text{Mo}$ or W , $R = \text{Cy}$; $M = \text{W}$, $R = \text{iPr}$) compounds were prepared according to the literature.³ All other reagents were obtained from commercial suppliers and used without further purification.

Sealed NMR tubes were prepared by connecting an NMR tube to a Kontes vacuum adapter via a Cajon joint, freezing the NMR tube in liquid nitrogen, and flame-sealing the tube with an oxygen/propane torch. "Glass bomb" refers to a cylindrical, medium-walled Pyrex vessel joined to a Kontes K-826510 high-vacuum Teflon stopcock.

Variable-Temperature NMR Spectroscopy of $M(\text{CO})_3(\text{PCy}_3)_2$ ($M = \text{Mo}$, W). Inside the drybox, $\text{Mo}(\text{CO})_3(\text{PCy}_3)_2$ (12 mg, 1.62×10^{-5} mol) was added to an NMR tube followed by 0.5 mL of toluene- d_8 . The tube was then flame-sealed under He, and the contents were analyzed by NMR spectroscopy on a Bruker AMX 500 MHz instrument. Samples of $\text{W}(\text{CO})_3(\text{PCy}_3)_2$, $M(\text{CO})_3[\text{P}(\text{Cy-}d_{11})_3]_2$ ($M = \text{Mo}$, W), and $\text{Mo}(\text{CO})_3(\text{PCy}_3)_2$ in a 1:1:1 *o*-xylene: Et_2O :hexane mixture were each prepared and studied in the same manner.

$[\text{W}(\text{CO})_3(\text{PiPr}_3)_2](\mu\text{-N}_2)$ (1). A 50 mL glass bomb was charged with $\text{W}(\text{CO})_3(\text{PiPr}_3)_2$ (204 mg, 3.47×10^{-4} mol) followed by 15 mL of toluene in the drybox. The solution was flushed with N_2 on a vacuum line by evacuating and then backfilling with N_2 two times. The yellow-brown solution was held at room temperature for 4 h, being backfilled with N_2 once more after the first 2 h. The solution was concentrated to 8 mL under vacuum, during the course of which a small amount of orange powder precipitated, which was subsequently redissolved by warming the solution. Inside the drybox, the yellow-brown solution was layered with 6 mL of hexane. Orange block crystals of **1** were isolated in 66% yield (139 mg) upon cooling this solution to -35 °C. ^1H NMR (C_6D_6): δ 2.30 (m, 12H, CH), 1.20 (m, 72H, CH_3). $^{13}\text{C}\{^1\text{H}\}$ NMR (C_6D_6): δ 211.42 (t, $J_{\text{CP}} = 5.3$, CO), 210.12 (t, $J_{\text{CP}} = 6.5$, CO), 28.17 (vt, $J_{\text{CP}} = 9.4$, CH), 20.25 (s, CH_3). $^{31}\text{P}\{^1\text{H}\}$ NMR (C_6D_6): δ 40.15 (s, $J_{\text{PW}} = 276.6$). IR (KBr): $\nu_{\text{CO}} = 1946$ (s), 1857 (sh), 1836 (br) cm^{-1} . Anal. Calcd for $\text{C}_{42}\text{H}_{84}\text{N}_2\text{O}_6\text{P}_4\text{W}_2$: C, 41.87; H, 7.03. Found: C, 42.22; H, 7.27.

$\text{W}(\text{H})(\text{CO})_3(\text{PiPr}_3)_2(\text{BF}_4)$. The complex $\text{W}(\text{CO})_3(\text{PiPr}_3)_2$ (151 mg, 2.57×10^{-4} mol) was dissolved in 8 mL of toluene in a 50 mL flask inside the drybox. A diluted solution of $\text{HBF}_4 \cdot \text{OEt}_2$ (40%, 259 mg, 6.40×10^{-4} mol, 2.5 equiv) in 5 mL of Et_2O was then added dropwise with stirring. The dark purple solution turned dark yellow over the course of the addition. The solution was allowed to stir at 25 °C for 1 h, during which a small amount of yellow precipitate formed. The volatile materials were removed under vacuum, leaving a dark yellow powder. This was washed with hexanes (2×5 mL) and then extracted with 10 mL of toluene. The yellow-brown solution was filtered, the filtrate was reduced to 5 mL under vacuum, and the concentrate was layered with 5 mL of hexane. Cooling this solution to -30 °C afforded yellow crystals of $\text{W}(\text{H})(\text{CO})_3(\text{PiPr}_3)_2(\text{BF}_4)$ (108 mg, 62% yield). This compound can also be synthesized by following this procedure using **1** as the starting material rather than the agostic complex. ^1H NMR (C_6D_6): δ 2.51 (br m, 6H, CH), 1.15 (br m, 36H, CH_3), -6.06 (m, 1H, W–H). $^{13}\text{C}\{^1\text{H}\}$ NMR (C_6D_6): δ 208.56 (br, CO), 207.15 (t, $J_{\text{CP}} = 6.8$, CO), 25.43 (d, $J_{\text{CP}} = 21.4$, CH), 19.73 (s, CH_3). $^{31}\text{P}\{^1\text{H}\}$ NMR (C_6D_6): δ 45.5 (br AB pattern). IR (KBr): $\nu_{\text{WH}} = 2023$ (m), $\nu_{\text{CO}} = 1920$ (s), 1913 (sh), 1883 (s) cm^{-1} . IR (toluene): $\nu_{\text{WH}} = 2002$ (s), $\nu_{\text{CO}} = 1906$ (br), 1889 (br), 1872 (br) cm^{-1} . This complex was not stable in the solid state at room temperature, and thus a satisfactory elemental analysis could not be obtained.

NMR and Crystal Growth of $\text{W}(\text{CO})_3(\text{PCy}_3)_2(\eta^2\text{-C}_2\text{H}_4)$ (2). The complex $\text{W}(\text{CO})_3(\text{PCy}_3)_2$ (19 mg, 2.29×10^{-5} mol) was added to a 7 in. J. Young NMR tube followed by 0.5 mL of C_6D_6 , forming a dark purple solution. On a vacuum line, the solution (only) was frozen in liquid N_2 and evacuated after which it was backfilled with 1 atm of ethylene. The solution became yellow immediately upon thawing and was analyzed by NMR spectroscopy. In a separate experiment, pale yellow crystals were grown by slowly cooling in a freezer a nearly saturated toluene solution of **2** under N_2 in a Schlenk flask placed inside a Dewar flask. ^1H NMR (C_6D_6): δ 2.44 (br, 6H, Cy), 2.36 (br s, 4H, C_2H_4), 2.17 (br m, 12H, Cy), 1.68 (m, 24H, Cy), 1.26 (m, 24H, Cy). $^{13}\text{C}\{^1\text{H}\}$ NMR (C_6D_6): δ 212.88 (t, $J_{\text{CP}} = 6.4$, CO), 209.49 (t, $J_{\text{CP}} =$

(56) Schenk, W. A.; Baumann, F.-E. *Chem. Ber.* **1982**, *115*, 2615.

(57) Burdett, J. K.; Downs, A. J.; Gaskill, G. P.; Graham, M. A.; Turner, J. J.; Turner, R. F. *Inorg. Chem.* **1978**, *17*, 523.

(58) (a) Sato, M.; Tatsumi, T.; Kodama, T.; Hidai, M.; Uchida, T.; Uchida, Y. *J. Am. Chem. Soc.* **1978**, *100*, 4447. (b) Tatsumi, T.; Tominaga, H.; Hidai, M.; Uchida, Y. *J. Organomet. Chem.* **1980**, *199*, 63.

(59) Lawless, G. A. Private communication (see also footnote 31 in ref 51).

(60) Kubas, G. J.; Jarvinen, G. D.; Ryan, R. R. *J. Am. Chem. Soc.* **1983**, *105*, 1883.

(61) Barbeau, C.; Dubey, R. J. *Can. J. Chem.* **1973**, *51*, 3684.

(62) Schenk, W. A.; Karl, U.; Horn, M. R. *Z. Naturforsch., B* **1989**, *44B*, 1513.

(63) Blomberg, M. R. A.; Siegbahn, P. E. M.; Svensson, M. *J. Phys. Chem.* **1994**, *98*, 2062.

(64) Haynes, C. L.; Armentrout, P. B. *Chem. Phys. Lett.* **1996**, *249*, 64.

6.4, CO), 28.60 (br t, $J = 4.2$, CH₂CH₂), 27–39 (Cy). ³¹P{¹H} NMR (C₆D₆): δ 19.60 (s, $J_{PW} = 227$).

Reactions of W(CO)₃(PR₃)₂ with PhSiH₃. (a) W(CO)₃(PCy₃)₂(H)(SiH₂Ph) (3**).** W(CO)₃(PCy₃)₂ (12 mg, 1.45×10^{-5} mol) was dissolved in 0.5 mL of toluene-*d*₈ in the drybox. Phenylsilane (1.9 μ L, 1.54×10^{-5} mol) was then added to the purple solution, which immediately turned brown. The solution was transferred to an NMR tube which was flame-sealed under He. The solution was bright yellow on cooling (-30 °C) and converted back to brown on rewarming. The reaction mixture was investigated by ¹H and ³¹P{¹H} NMR spectroscopy. The resonances for the oxidative-addition product W(CO)₃(PCy₃)₂(H)(SiH₂Ph) were broad at 0 °C and sharpened on cooling to -30 °C. Further broadening at lower temperatures was attributed to the slow-exchange regime being approached for the intramolecular ligand exchange in the 7-coordinate complex. ¹H NMR (toluene-*d*₈, -45 °C): δ 8.14 (d, $J = 7.1$, 2H, *o*-Ph), 7.33 (t, $J = 7.4$, 2H, *m*-Ph), 7.19 (t, $J = 7.7$, 1H, *p*-Ph), 5.79 (s, $J_{SiH} = 176.8$, 2H, SiH), 2.35 (br, 6H, Cy), 1.77 (br, 12H, Cy), 1.61 (br, 24H, Cy), 1.23 (br, 24H, Cy), -4.51 (t, $J_{HP} = 14.9$, $J_{HW} = 28.2$ (determined in an ¹H{³¹P} NMR experiment), 1H, WH). ³¹P{¹H} NMR (toluene-*d*₈, -20 °C): δ 31.7 (br s). IR (toluene, 25 °C): $\nu_{CO} = 1973, 1898, 1854$ cm⁻¹.

(b) W(CO)₃(PiPr₃)₂(H)(SiH₂Ph) (4**).** This compound was prepared by the same method used for the analogous PCy₃ complex. ¹H NMR (toluene-*d*₈, -30 °C): δ 8.02 (d, $J = 7.1$, 2H, *o*-Ph), 7.32 (t, $J = 7.4$, 2H, *m*-Ph), 7.14 (t, $J = 7.7$, 1H, *p*-Ph), 5.66 (d, $J_{HH} = 1.8$, $J_{SiH} = 180.2$, 2H, SiH), 2.32 (m, 6H, CH), 1.10 (vq, $J = 6.8$, 36H, CH₃), -4.90 (dt, $J_{HP} = 14.9$, $J_{HH} = 1.8$, $J_{HW} = 29.6$, 1H, WH). ³¹P{¹H} NMR (toluene-*d*₈, -30 °C): δ 32.9 (s, $J_{PW} = 207$). IR (toluene, 25 °C): $\nu_{CO} = 1977, 1962, 1902$ cm⁻¹.

(c) [W(CO)₃(PiPr₃)₂(μ -SiHPh₂)]₂ (5**).** In the drybox, W(CO)₃(PiPr₃)₂ (402 mg, 6.83×10^{-4} mol) was added to a 50 mL bomb, followed by 10 mL of toluene. Diphenylsilane (380 μ L, 2.05 mmol, 3 equiv) was then added by syringe to the purple solution, which immediately turned dark brown. The solution was heated in a 60 °C oil bath for 6 h, during which the solution turned dark red. Inside the drybox, the volatile materials were removed under vacuum, leaving a dark red oil, which was triturated with hexane three times and then washed with hexane (3 \times 10 mL, dark red to yellow washings). Drying under vacuum afforded a tan powder. This crude product was dissolved in 16 mL of toluene, the solution was layered with 16 mL of hexane, and the mixture was placed in a -30 °C freezer. Orange crystals were isolated in 34% yield (142 mg). The sample for elemental analysis was recrystallized a second time from THF/hexane at -30 °C. ¹H NMR (THF-*d*₈): δ 7.58 (m, 8H, Ph), 7.21 (m, 12H, Ph), 2.68 (m, 6H, CH), 1.22 (dd, $J = 13.9, 7.2$, 36H, CH₃), -7.26 (m, 2H, WH). ¹³C{¹H} NMR (THF-*d*₈, 5 °C): δ 218.18 (d, $J_{CP} = 16.5$, CO), 202.65 (d, $J_{CP} = 5.7$, CO), 144.90 (s, Ph), 136.98 (s, Ph), 129.51 (s, Ph), 127.64 (s, Ph), 31.56 (d, $J_{CP} = 22.9$, CH), 20.20 (s, CH₃). ³¹P{¹H} NMR (THF-*d*₈, 0 °C): δ 36.7 (s, $J_{PW} = 234$). ²⁹Si NMR (THF-*d*₈, -20 °C): δ 146.3 (br d, $\nu_{1/2} = 23$

Hz, $J_{SiH} = 52$). IR (KBr): $\nu_{CO} = 1977, 1909, 1874$ cm⁻¹. Anal. Calcd for C₄₈H₆₄O₆P₄Si₂W₂· $\frac{1}{2}$ C₄H₈O: C, 48.23; H, 5.60. Found: C, 47.85; H, 5.29.

Single-Crystal X-ray Diffraction Studies. A crystal of either **1** (orange cube), **2** (yellow cube), or **5** (red block) was mounted on a glass fiber using silicone grease from a pool of mineral oil, bathed in Ar. The crystal was immediately mounted on the goniostat and cooled under a N₂ stream. A summary of crystallographic data is given in Table 2. Data were obtained on an Enraf-Nonius CAD4 (**1**), a Siemens R3m/V (**2**), or a Siemens P4 (**5**) diffractometer using graphite monochromated Mo K α ($\lambda = 0.71073$ Å) radiation. Intensities were corrected for Lorentz and polarization effects, and empirical absorption corrections based on a set of ψ scans were applied. The structures were solved by direct methods and expanded in subsequent Fourier syntheses. Calculations were carried out using Siemens' SHELXTL. The ethylene H atoms in **2** were located and refined with all their related 1,2 and 1,3 distances restrained to be equal. Each H atom was also given an isotropic displacement parameter equal to 1.2 times the equivalent isotropic displacement parameter of the atom to which it was attached. All other H atoms in all three structures were placed in calculated positions, refined using a riding model, and given isotropic displacement parameters equal to 1.2 (CH, CH₂) or 1.5 (CH₃) times the equivalent isotropic displacement parameter of the atoms to which they were attached. Additionally, methyl H atomic positions were allowed to rotate about the adjacent C–C bond. The hydride H atom in **5** was not located. Full-matrix least-squares refinement of all data against F^2 of the quantity $\sum w(F_o^2 - F_c^2)^2$ was used to adjust the positions and anisotropic thermal parameters of all non-hydrogen atoms. All peaks in the final difference maps >1 e/Å³ were located near a tungsten atom.

Acknowledgment. This work was supported by the Department of Energy, Office of Basic Energy Sciences, Division of Chemical Sciences, and the Laboratory Directed Research and Development Office at Los Alamos. We are most grateful to David M. Barnhart for performing the initial X-ray structure determination of complex **2** (data were subsequently re-refined against F^2 by J.C.B.) and to Lori Van Der Sluys and G. R. K. Khalsa for NMR investigations. We also thank Mike Heinekey for helpful discussions concerning the temperature-dependent behavior of the agostic complexes.

Supporting Information Available: X-ray crystallography files, in CIF format, for the structure determinations of complexes **1**, **2**, and **5** are available on the Internet only. Access information is given on any current masthead page.

IC960870A